Chemical Engineering Journal 528 (2026) 172251

Contents lists available at ScienceDirect

Chemical Engineering Journal

journal homepage: www.elsevier.com/locate/cej

Review

Direct/indirect strategies on engineering extracellular electron transfer of anode electrodes in microbial electrolysis for hydrogen production and pollutants removal: A review

Seyed Masoud Parsa [a], Huu Hao Ngo [a,*], Bing-Jie Ni [b], Xinbo Zhang [c], Ying Liu [c], Li Luo [d], Hui Cheng [e], Wenshan Guo [a,*]

[a] Centre for Technology in Water and Wastewater, School of Civil and Environmental Engineering, University of Technology Sydney, NSW, 2007, Australia
[b] Water Research Centre, School of Civil and Environmental Engineering, The University New South Wales, Sydney, NSW, 2052, Australia
[c] Tianjin Key Laboratory of Aquatic Science and Technology, Tianjin Chengjian University, Jinjing Road 26, Tianjin, 300384, China
[d] Key Lab of Environmental Engineering, Shaanxi Province, Xi'an University of Architecture and Technology, No. 13, Yanta Road, Xi'an, 710055, China
[e] School of Environmental and Chemical Engineering, Shanghai University, 333 Nanchen Road, Shanghai, 200444, China

ARTICLE INFO

Keywords:
Carbon-based anodes
Electrode modification
Surface treatment
Biofilm engineering
Biohydrogen production
Wastewater treatment

ABSTRACT

Anode electrodes are at the focal point of developing microbial electrochemical cells (MECs) for hydrogen production. The extracellular electron transfer (EET) of microorganisms at the interface of anodes and biofilm is the driving force of MECs. This signifies, the role of designing high-performance anodes to maximize the rate of EET and hydrogen production. In this paper, a thorough discussion on the adopted strategies over the past 15 years on anodes to improve biohydrogen production and pollutant removal was presented. Importantly, these strategies categorized as the direct and indirect methods. For the first scenario, the surface of anodes was subjected to various modification methods such as utilizing biochars, nanomaterials, polymers etc. while in the second scenario, the performance of electrodes improved by implementing indirect strategies such as regulating electrodes ratio/spacing, acclimation, electrodes arrangement, magnetic field etc. just to name a few. It was realized that, employing functional materials are at the spotlight of improving anode electrodes while methods such as applying electrical shocks or magnetic field are in early stages. The pros and cons and synergistic impacts on concurrent utilization of methods were also analyzed. Finally, current bottlenecks and future directions for implementing fundamental studies to tackle existing challenges were suggested.

1. Introduction

In the beginning of the new millennium, the United Nations (UN) declared important action plans such as the Millennium Development Goals (MDGs) and the Sustainable Development Goals (SDGs) toward protecting the blue planet and our society [1–3]. These action plans consist of several goals which can be generally divided into two main categories. The first one mainly focuses on human-related issues such as hunger, inequality, education, etc. The second one mainly focused on environmental-related issues such as reducing greenhouse gases emissions, water and sanitation, clean energy, and protecting life in water, just to name a few. Importantly, achieving some of these goals can directly and indirectly assist in the realization of other goals such as Goal 7 of the SDGs " Affordable and Clean Energy for All" which related to more than three-fourths of the other 174 targets of the SDGs [4,5]. Surprisingly, wastewater can be considered as a double-edged sword as it can be considered as one of the major pollution sources of water resources and transboundary rivers [6,7], while on the other side of the coin, it also contains a huge amount of energy and resources in the form of organic matter which can be harnessed and recovered by employing microbial electrochemical technologies (METs). The MET schemes such as microbial fuel cells (MFCs), microbial electrolysis cells (MECs), and microbial electrosynthesis (MES) are proposed as a dual-purpose method in this context because they can generate bioenergy as the main product when employed for wastewater treatment. The main components in METs are almost the same, including the anode and cathode electrodes, a membrane separator (in the case of double chamber geometry), and a power supply (when the main product is not

* Corresponding authors.
E-mail addresses: ngohuuhao121@gmail.com (H.H. Ngo), wguo@uts.edu.au (W. Guo).

https://doi.org/10.1016/j.cej.2025.172251
Received 21 September 2025; Received in revised form 19 December 2025; Accepted 23 December 2025
Available online 24 December 2025

electricity). Importantly, MEC is one of the latest technologies in this field starting in 2006 [8,9] with a focus on producing hydrogen as a clean fuel and concurrently treating wastewater. The general principle of MECs is as follows: Electro-active microorganisms accumulate on the surface of the anode electrode and break down wastes or organic materials into electrons, protons, and carbon dioxide. Afterwards, the microorganisms transfer electrons and protons to the surface of the anode and the MEC's solution, respectively. By applying a small voltage, electrons are transferred to the cathode where they combine with protons that results in biohydrogen production through the hydrogen evolution reaction (HER). This technology is an interesting strategy for realizing important SDGs such as Goal 6 (water and sanitation) and Goal 7 (clean and affordable energy). Therefore, technology advancements in this field could be considered as an important step toward realizing the SDGs, which is the reason why researchers have performed colossal number of reviews in the wide spectrum of METs. In this regard, anode electrode plays a crucial role in the MET particularly for producing bioelectricity and biohydrogen through MFC and MECs, since it is considered as the driving force of the process. Indeed, the anode mechanism of operation of anode in MFCs and MECs in some aspects could be considered similar.

Current reviews on MEC can be categorized in several branches where with the main focus has been on presenting a general overview on recent progress in MEC systems [10–25]. The terms "general overview" means that in the above-referenced reviews current advances on MEC were reviewed by examining all components/parameters including anode/cathode electrodes, design procedures, system parameters, and so on. Although the above reviews have presented valuable insights on the recent progress in this context, however, they could not provide an in-depth analysis as they reviewed the recent advances on all MEC components. The second interesting topic highlighted in the literature was on the applied materials with an explicit focus on the cathode such as various types of catalysts [26–35] and biocathodes [36–39] while the integration of MEC with other technologies like anaerobic digestion (AD), MFC, dark fermentation etc. comes as the third topic [40–47]. Besides of these three categories that a majority of reviews focused on them, other subjects related to the MEC such as utilizing various substrates [48–50], suppressing methanogens [51–53], biofilm and exoelectrogenic routes [54–56], reactor configuration [57,58], scale-up challenges [59,60], source of power supply [61], hazardous removal [62] were reviewed in the literature. As points out above, the anode conditions and applications in MFCs are somehow like MEC, thus, it is crucial to highlight review papers on the anode electrode in MFC. However, it is important to point out that as MECs operate under an external applied voltage, they generally result in higher current densities and change electron-transfer kinetics at the anode–biofilm interface as well as microbial community structure and redox activity. Moreover, although anode MEC anodes are maintained under strictly anaerobic conditions, MFC anodes could experience anoxic environments [63] (e.g., air-cathode configurations) due to oxygen diffusion through the cathode. Ma and co-workers [64] highlighted the utilization of various types of materials utilized as anode electrode in MFCs including carbonaceous materials, polymers and metallic/metal oxide- anodes. The main focus of the article was on the material science approach and how a wide range of modifiers can improve the power density of MFC. Similarly, Fan et al. [65] from an applied materials viewpoint, reviewed various carbon-based anodes in MFCs and mainly focused on categorization of carbon materials at different dimensions and diverse compositions. In an interesting review paper, Li and Cheng [66] focused on the impact of functional groups in the development of the biofilm on the anode's surface in MET systems. The article critically reviewed different stages in biofilm formation and the roles and effects of different functional groups in every stage including microorganism adhesion, bacterial growth and the electrochemical characteristics of the biofilm.

Despite these contributions, most reviews have primarily emphasized on various types of applied materials in anodes. Moreover, the effect of MEC's operational parameters on the anode electrodes not only in MECs but in METs has not fully understood. Importantly, general crucial design guidelines on using anode in the MEC, considering numerous physical parameters/modifications, including the electrode thickness, electrodes spacing, electrode geometry and ratios, utilizing additive nanomaterials, the acclimation procedure, etc. just to name a few, are missing in the literature.

To address these gaps, this review aims to deliver a thorough, critical assessment of the entire spectrum of internal and external factors affecting anode electrodes in MECs. It highlights both physical and chemical modifications to anodes, evaluating their positive and negative effects on system performance. Moreover, it highlights the operational parameters and their pivotal roles in the performance of the anode. Furthermore, the crucial role of utilizing advanced biocompatible nanostructures on carbon materials to boost the extracellular electron transfer (EET) on anode electrodes has not been outshined. It is worth to be reminded that the wide range of insights on engineering anodes in present review could also be applied in anodes for MFCs. Fig. 1 schematically summarizes the engineering strategies and design criteria for carbon-based anodes in MECs discussed in this paper.

2. Mechanisms of extracellular electron transfer (EET) in anode

The process that microorganisms break down the organic matter within wastewater is the first step and one of the important driving forces of MECs which leads to the production of electrons and protons. Subsequently, through the extracellular electron transfer (EET) mechanism the generated electrons by anode-respiring bacteria (ARB) are transferred to the anode electrode. Briefly, the ARBs act as electroactive microorganisms that couple intracellular substrate oxidation with EET to the anode. During metabolism, ARBs oxidize organic compounds as substrate (e.g. glucose, acetate, or lactate) to generate electrons and protons where the electrons are transferred to the anode either directly through outer-membrane cytochromes and conductive pili or indirectly via soluble redox mediator. This process effectively links microbial catabolism with electrode reduction and forms a biochemical basis for current generation in microbial electrochemical systems. There are three possible mechanisms for EET of ARBs inside MEC named: direct contact, the soluble shuttle mechanism and solid conductive network. Although the contribution of each method was not exactly clear, by discussing on mechanisms, we would draw a conclusion on the importance of each method as it illustrated in Fig. 2. It is important noting that the EET has been subjected to study for a wide range of applications not only in METs but also in Fenton-like processes, CO2 fixation, and chemical degradation, just to name a few [67–69].

In direct contact EET, a single layer ARBs sets on the surface of the anode and transfers electron from outer membrane to the electrode. Upon reaching the electrons on the surface of electrode, an electrochemical process releases electrons on the conductive electrode (extracellular matrix). This process -which plausibly is reversible because of previous observations in transferring electrons in cytochromes [70]- occurs between outer membrane protein and the electrode.

The soluble shuttle mechanism is based on the fact that many microorganisms and molecules in the environment are capable to act as an electron donor and acceptor between cells and solid hosts through diffusive transport respectively. Plenty of researches in the last two decades on several families of bacteria such as *Shewanella*, *Pseudomonas*, *Escherichia* to name a few, has been conducted with this unique feature [71–74]. One of the greatest advantages of the shuttle mechanism over direct contact is that it can generate more than just a single monolayer filament; rather, it can activate via multiple-biofilm layers which leading to higher rate of electron transfer to the anode. However, one of the main obstacles through this mechanism is that it can be limited through the distance of biofilm form electrode ascribe to diffusive limitation. It is important to note that, the kinetics of mediated electron transfer depend on the mediator diffusion coefficient and its redox potential. This means

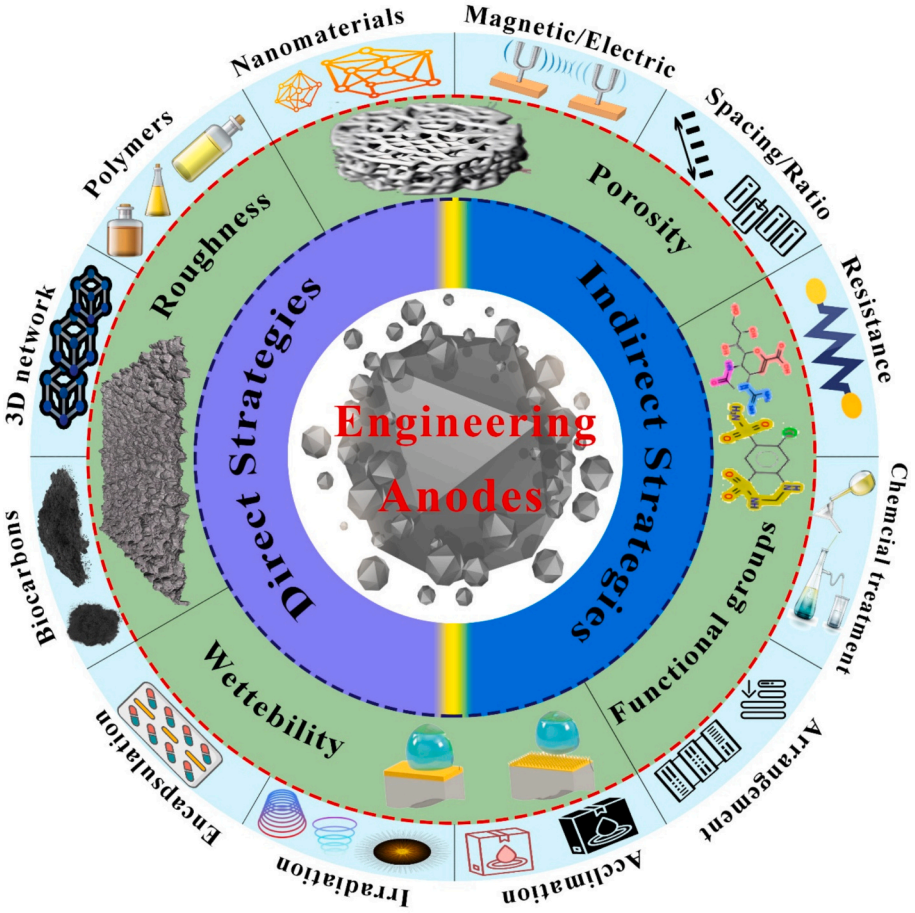

Fig. 1. Influential parameters and adopted strategies on engineering anode electrodes in MEC.

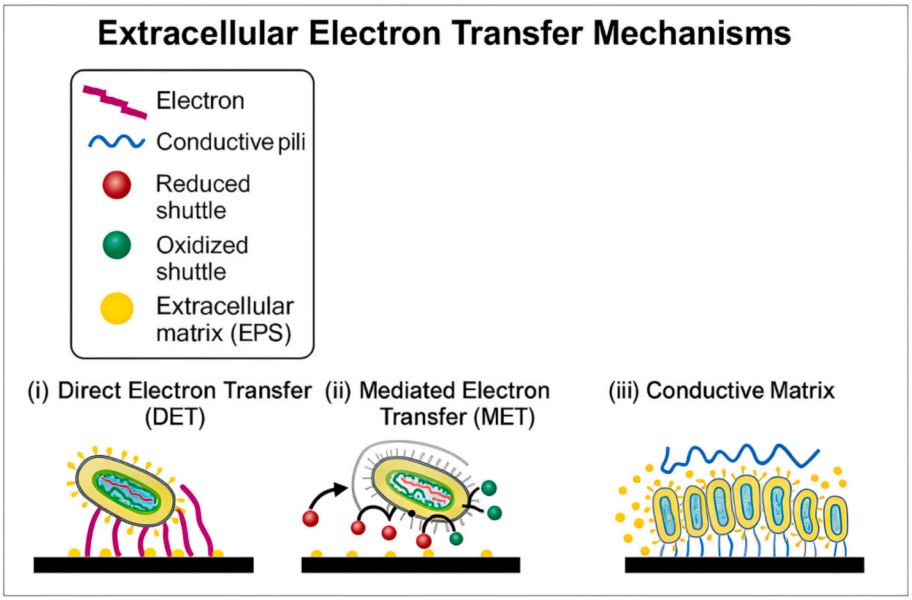

Fig. 2. Possible mechanisms of extracellular electron transfer (EET).

that a higher diffusion coefficient (and concentration) increases mediator flux to the electrode, hence, it raises the mass-transport limited current, whereas low sequestration in the biofilm imposes a diffusion bottleneck. Moreover, mediator's formal redox potential determines the thermodynamic driving force for electron transfer between donors (microorganism) and acceptors (electrode) which controls the heterogeneous electron transfer rates via overpotential and Marcus/Butler–Volmer behavior. In this regard, if the shuttle potential is not well aligned with the microbial redox pool and electrode potential, mediator cycling and current generation are inefficient. Collectively, these

parameters whether a system is mass-transport limited, thermodynamically constrained, or kinetically limited [75–77].

The third mechanism called the solid conductive network (SCN) by ARBs, is considered to be responsible for EET through a solid conductive/semi-conductive material for transferring electrons [78,79]. Given the features of the possible exopolymeric materials generated by ARBs, the SCN is likely to act as a semi-conductive material rather than a conductor. Previous experiments [80,81] and mathematical simulations [82] have elucidated that nanowires connect bacteria with other parts of biofilms, supporting the assumption that other solids in the extracellular biofilm network are also electrically conductive. To date, limited understanding on the conductivity of bulk SCN –as one of the most important parameters- has been achieved. Although some studies suggested that cytochromes could be responsible for the conductivity of the SCN biofilm, recent finding proved that this is an incorrect assumption-at least for *Geobacter sulfurreducens*- when inactivation of cytochrome results in no changes in conductivity of SCN biofilm, hence, protein nanowires play the main role [83]. It is important to point out the difference between nanowires and EPSs in biofilm conductivity. The main difference between them could be defined as protein nanowires (e.g. conductive pilin monomers or multi-heme *c*-type cytochromes) act as filamentous electron conduits that support long-range electron transport between cells and to electrodes while EPS (e.g. polysaccharides, proteins, DNA and associated redox moieties) forms the matrix that embeds cells and conductive components that facilitates short-range charge and binding redox-active moieties. Thus, it affects mass transport and local dielectric properties. However, it worth to point out that EPS alone is generally less conductive than organized protein nanowires. Experimental and structural studies provide evidence for metallic-like conductivity in *Geobacter* pili and the importance of aromatic amino acids and dense π-stacking for long-range conduction [84–86].

Moreover, *c*-Type cytochromes play a central role in mediating EET between cells and electrodes. In *Geobacter. S*, outer-membrane cytochromes such as OmcZ and OmcB facilitate direct electron transfer from the periplasm to the anode surface, while OmcZ forms conductive biofilm matrices that enhance long-range electron transport [87]. In *Shewanella. O*, multiheme cytochromes MtrC and OmcA form a transmembrane complex which transfers electrons from inner membrane quinol pool through periplasmic intermediates to the cell exterior, where they reduce solid electrodes or metal oxide [88]. These cytochromes thus act as molecular electron conduits that link intracellular redox reactions to external electron acceptors.

Collectively, the third mechanism could be considered as the main mechanism for EET in MECs, even though the two other methods may have contribute. For the first mechanism, in an ideal condition (the best biofilm conditions and transferring all electrons) the highest current could reach to 0.24 A/m^2. For the second mechanism, due to diffusive limitations, the rate of current density is between 0.13 and 0.57 (in ideal conditions) A/m^2 which is still 20 times smaller than the observed values of the third mechanism for current density. Thus, regarding the high-current obtained by the third approach (>8 A/m^2) the main mechanism which should be brought into spotlight to maximize EET is the SCN biofilm [89].

3. Types of carbon-based materials as anode electrode

Carbon materials, due to their exceptional characteristics are extensively applied in the wide-spectrum of energy and environmental schemes such as metal-ion batteries [90], metal-air batteries [91], supercapacitors [92], organic/inorganic contaminant absorbents in soil, air, and aqueous media [93], CO2 capture [94], novel perovskite solar cells [95], desalination and interfacial evaporation [96], just to name a few. Indeed, carbon-based materials due to their unique features such as biocompatibility, high specific surface area, earth-abundance, low-cost, tunable structure and versatility, widely applied in microbial electrochemical systems, with anode at the top of their applications. A wide range of carbon materials [97] with different structures (Fig. 3) are used in METs, however, as the anode of METs four types were widely used which are carbon felt [98–103] carbon cloth [104–107], graphite-based electrodes [108–113] and carbon paper/fibers [114–116].

- Carbon Cloth is a flexible, woven material with a high surface area which widely used due to its durability and ease of microbial colonization to support strong biofilm formation and efficient electron transfer.
- **Carbon Felt** is a fibrous, three-dimensional structure with a large surface area, enhancing microbial attachment and electron transfer.
- **Graphite-based (Rods/Plates/Brushes) electrodes**: Graphite-based electrodes are dense, durable, and highly conductive family of carbon materials. While they have a lower surface area than some other carbon materials, they offer stability and exhibited promising results in long-term operation.
- **Carbon Paper**: Known for its high conductivity and relatively flat structure, carbon paper allows easy handling and can be treated to increase surface roughness, which aids microbial adhesion.

It is worthy to be noted that there are other types of carbon-based materials utilized as anode like granular, carbon mesh, reticulate carbon etc., but these four categories are the most utilized carbon materials as the anode in bioelectrochemical systems.

From the beginning development of MEC systems in the past 15 years, numerous approaches have been employed to improve the performance of anode electrodes toward superior EET and biofilm formation. These approaches developed in a wide spectrum from geometry/physical optimization to regulating different internal parameters of MEC. It is important to remind that carbon-based materials, attributed to the aforementioned features are not only used as the anode electrode but they widely used as the electrocatalysts in other MET schemes [117].

3.1. Improving the EET process of anode electrodes

As mentioned above, the reason for using carbon materials as anode electrodes is their specific features for biofilm formation and efficient EET. Conventionally, for further improvement of EET in carbon electrodes, several methods in most experiments such as washing with various acids and bases, annealing, steam or CO_2 activation etc. have been adopted. Briefly, these conventional methods change the surface chemistry, microbial affinity and porosity of anode material. For instance, washing with acids or oxidative agents introduce oxygen-contain functional groups (e.g. –OH, –COOH) which augment hydrophilicity and provide surface redox sites to promote microbial adhesion and interfacial electron transferring. Moreover, applying physical activation such as CO2, enlarges surface area by creating micro-/mesopores that increase active area for biofilm formation. However, in recent years, effective approaches like utilizing biocompatible nanostructured materials or irradiating with ultraviolet light have showed promising results, need further investigations. Moreover, in several novel approaches, biocompatible structures such as stand-alone anode electrodes (without carbon electrodes as the substrate) were successfully utilized. Since the conventional methods in the previous studies have been thoroughly reviewed, here, we will just highlight the recently applied methods to boost EET in bioelectrochemical schemes.

3.1.1. Utilizing biocompatible functional materials

Very recently, numerous studies have focus on improving the EET in BESs on anode electrodes through different forms of hybrid materials in the form of hydrogels, powder, or liquid such as doping sulfur on few-layer MXene [118], anchoring Co_9S_8–MoS_2–$CoMo_2S_4$ on 2D nanosheets [119], co-doping by $NiFe_2S_4$ and Fe_3O_4 and magnetite [120], utilizing hybrid composite such as polypyrrole@CNTs-MoSe2 [121] among others. For instance, sulfur doping modifies the electronic structure of $Ti_3C_2T_x$ MXene by providing surface defects and

Fig. 3. Various types of carbon materials used in microbial electrochemical technologies.

heteroatomic sites which enhance electrical conductivity and results additional redox-active centers for microbial species for exchanging electrons. Moreover, it improves hydrophilicity and chemical affinity of microbial outer-membrane cytochromes. Collectively, these modifications lead to promote strong biofilm adhesion and efficient charge transport at the interface of cells and electrode. Furthermore, 2D layered structures like MXene, exposes abundant active edges and facilitate the adsorption and regeneration of soluble redox mediators (e.g., flavins or quinones) which results in accelerating EET compared to pristine carbon materials. Wang e al. [122] through a simple pyrolysis process (Fig. 4a) used polyvinylpyrrolidone as dispersant to encapsulate the iron carbide to prepare a core-shell structure which coated on the surface of carbon felt for improving EET. Their finding indicated a substantial enhancement in BES current density due to the exceptional features of core-shell structure such as high-surface area, optimizing community and biocompatibility leading the EET improvement (Fig. 4d). Moreover, Meng and co-workers. [123] integrated soft-template with seed-mediated epitaxy methods (Fig. 4a) to fabricate a nanocomposite by inducing ZIF-8/ZIF-67 to grow on PPy nanotubes following by carbonization that results in biomimetic grape-like composites (PNTs/ZIF-8/ZIF-67@NC) to coat on the surface of carbon felt. The modified electrode exhibited a significant lower internal resistance with higher current density due to facilitating the EET by hybrid structure as depicted (Fig. 4c). Importantly, ZIF-derived hierarchical composite by combining structural and compositional synergies boost multiple path electron by generating: (i) multiscale porosity (micro/meso/macro pores) that reduces tortuosity and separates ionic and molecular transport routes which leads to fast ion diffusion, (ii) conductive substructure -during pyrolysis- that create percolating electronic network which provide direct electron transfer and (iii) heteroatom self-doping which introduce redox-active centers and locally increase electronic density that augment interfacial charge transfer to microbes or mediators. The synergies between these features provide parallel channels for superior EET via continuous electronic network, generating 1D/filamentary bridges (CNTs or graphite ribbons), and redox mediator cycle inside pores. Zhu et al. [124] through a facile two-step method by in-situ polymerization and carbonization at 850 °C, coated bimetallic (Molybdenum and Tungsten) carbides on the surface of the carbon cloth as the anode of MFC (Fig. 5a). The findings showed significant improvement in power generation through Mo_2C-W_2C@carbon anode ascribe to high-efficient EET process described through four factors including: a) colossal number of bacteria with conductive pili in anodic biofilm, b) the enrichment of functional bacteria related to sulfur cycle in the microbial community, c) providing abundant active sites by the 3D hierarchical structure of Mo2C-W2C microspheres to promote the adsorption of flavin species, d) the synergies between various elements of multi-interface bimetallic heterostructures can adjust the electronic structure of the surface, leading to accelerate the EET (Fig. 5c).

Interestingly, Pan and colleagues [125] co-doped Zr, Fe, and N by using amino-modified zirconium (Zr) and Fe—Zr metal organic frameworks, followed by pyrolysis (Fig. 5b) as the standalone bioanode without using carbon as a substrate. The experiments highlighted a significant improvement in power generation for the co-doped Zr, Fe, N around 45 % which validated by DFT results. Moreover, they suggested three reasons for exceptional EET (Fig. 5d) in the co-doped electrode as (i) The hierarchical porous structure of Zr-based carbon skeleton provided abundant colonization sites for microorganisms that improved the adsorption capacity of substrate, performance of diffusion, and decreased the energy loss due to concentration polarization (ii) by introducing the Zr atoms the density of Fe atoms' local positive charge increased which leading to improve the DET process utilized through exoelectrogens via direct contact with nanowires or conductive flagella. (iii) The synergies of Fe and Zr atoms promoted the chemical adsorption of flavin compounds at the interface of bioanode, which leading to boost EET process by increasing the number of transferred electrons. In another words, Co-doping Zr-Fe-N modified electronic feature of bioanode in multiway through providing redox centers by Fe—N moieties that facilitate acceptance of electron form microbes outer-membrane while addition of Zr atoms prevent the agglomeration of atomically dispersed Fe particles; at the same time, it incorporated in nitrogen-rich carbon environment to change the local charge distribution and boost kinetic of electron transfer. Moreover, integration of Zr, Fe and N boost formation of defects, partial graphitization and electronic percolation. Altogether, these synergies results in increasing electroactive site

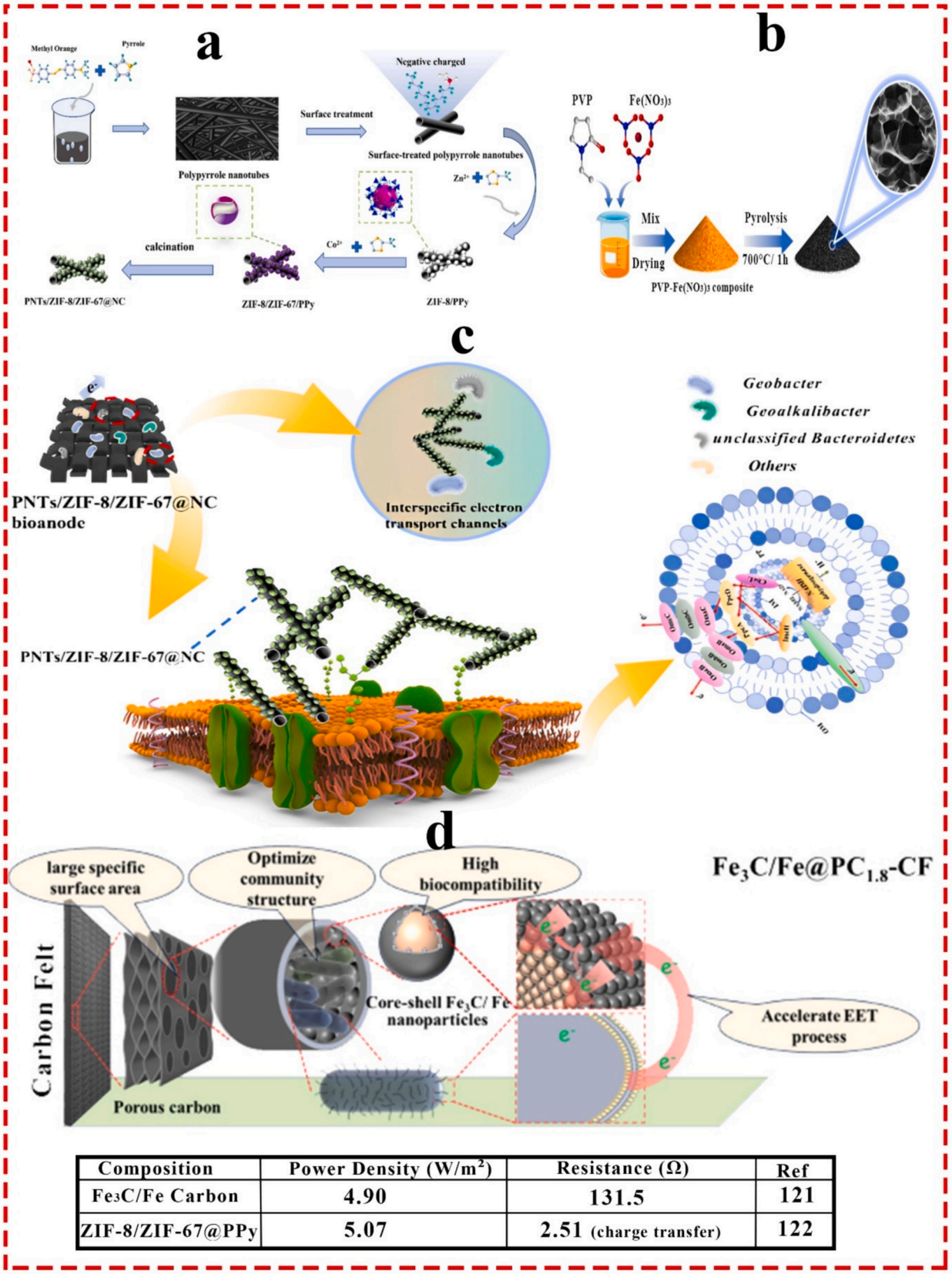

Composition	Power Density (W/m^2)	Resistance (Ω)	Ref
Fe3C/Fe Carbon	4.90	131.5	121
ZIF-8/ZIF-67@PPy	5.07	2.51 (charge transfer)	122

Fig. 4. a) Graphical diagram of the PNTs/ZIF-8/ZIF-67@NC preparation procedure. [123] reprinted with permission from Elsevier. b) Graphical diagram of Fe3C/ Fe@PCX preparation procedure. [122] reprinted with permission from Elsevier. c) Graphical illustration the existing EET pathways [123] reprinted with permission from Elsevier. d) The suggested mechanism for improved power production with Fe3C/Fe @PC1.8-CF anode in MFC [122] reprinted with permission from Elsevier.

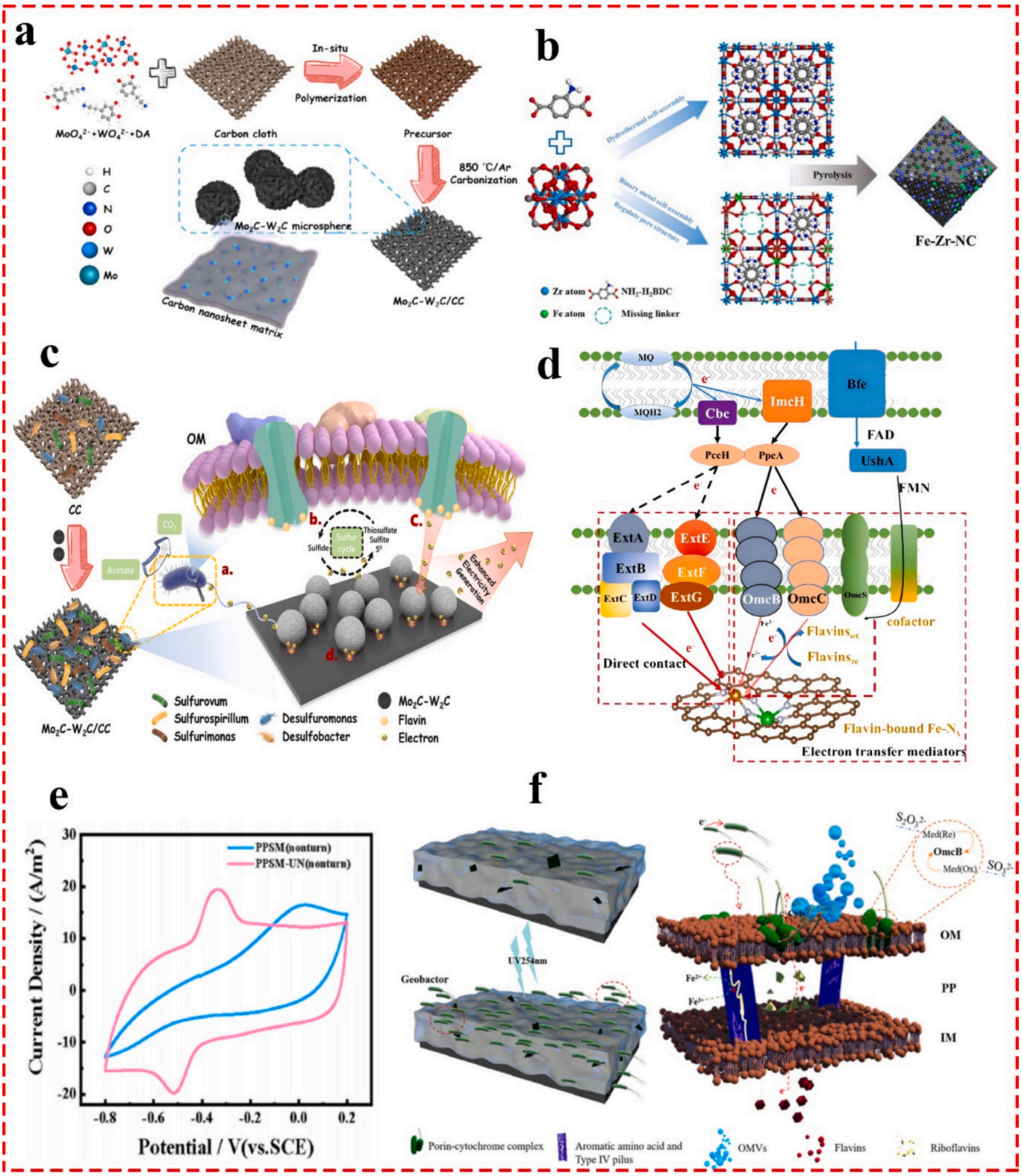

Fig. 5. a) Graphical illustration of Mo2C-W2C/CC preparation method used as anode in MFC [124] reprinted with permission from Elsevier. b) Graphical diagram of Fe-Zr-NC anode fabrication method. [125] reprinted with permission from Elsevier. c) The suggested mechanism of enhancing EET with the Mo_2C-W_2C [124] reprinted with permission from Elsevier. d) The plausible mechanism of EET for Fe-Zr-NC anode. [125] reprinted with permission from Elsevier. e) The CV graphs of PPSM and PPSM-UN under non-turnover condition [126] reprinted with permission from Elsevier. f) Schematic illustration of predicted map for electrons transfer pathway. (OM: outer membrane, PP: periplasm, IM: intermembrane.) [126] reprinted with permission from Elsevier.

density, improving electronic coupling to microbial redox proteins, and reduce the charge transfer resistance at the bioanode.

3.1.2. Irradiating by UV

Zhu et al. [126] prepared a hydrogel by in-situ polymerization of PEDOT-PSS, PAM, SA, and MXene (PPSM) on a conductive collector combined with ultraviolet irradiation and liquid nitrogen (PPSM-UN) freezing to enhance conductivity, porosity, and surface functionality to coat on the surface of carbon felt as MFC's anode. The PPSM-UN electrode showed higher electrochemical activity than the unmodified one (Fig. 5e). Furthermore, it had superior hydrophilicity and formed a wet 3D network when placed in the anolyte, which helped microbes grow and made it easier for them to release electrons. What's more, the PPSM electrode surface was negatively charged, causing repulsion between the electrode and electroactive microbes (mainly Gram-negative bacteria) that have outer membranes full of lipopolysaccharides. This repulsion made it harder for microbes to stick to the electrode. But when UV light was used, the PSS part of the PPSM-UN electrode which has many sulfonic groups could break apart or oxidize. This process could create positive charges or reactive radicals, all of which resulted in excellent EET (Fig. 5f).

3.1.3. Physical and geometrical modification

Besides the above-mentioned strategies on direct modifications of the electrode, there are some approaches that do not need to change the anode surface and interfaces chemistry; rather, they focused on modifying electrode performance through regulating the physical arrangements of electrodes such as utilizing several anodes instead of single electrode, stacked anodes, and regulating the ratio of anode to cathode. Moreover, the potential of employing different fabrication 3D anodes instead of using prepared anodes (listed in Section 3) using different family of materials have been reviewed [127–129]. It is important to note that one of the important advantages of using 3D fabrication methods is to precisely design an optimum structure to improve biofilm density and adhesion of microbial communities. For instance, Bian and co-workers [130], proposed to use 3D printed anode to improve the rate of EET and higher current generation in MFC. Their findings, revealed that, the MFC with 3D printed carbon anode generated 3.4 times (233.5 ± 11.6 $mW{\cdot}m^{-2}$) than system with pristine carbon cloth (69.0 ± 4.7 $mW{\cdot}m^{-2}$). It is important to note that, 3D printing fabrication is not only effective on carbon-based anode, but it is highly effective in metal-based anodes. For example, the same research group [131] showed that by fabricating a 3D printed copper-based anode delivered 6.45 ± 0.5 $mW{\cdot}m^{-2}$ current density in MFC which was ~12 higher than a copper mesh anode of similar design highlighted the role of highly ordered and open porous architecture on developing a dense microbial biofilm. In another study [132], it was examined a 3D porous carbon foam under laboratory experiments can obtained up to >20 $A{\cdot}m^{-3}$ currents which outperformed than the many 2D electrodes by orders of magnitude in volumetric performance.

4. Strategies for improving anode electrodes in MEC

4.1. Regulating electrode resistance

The internal resistance of electrodes in microbial electrochemical technologies can be categorized to three branches including (i) charge transfer resistance (R_{ct}), ionic diffusion resistance (R_{diff}), and ohmic resistance (R_{Ω}). The R_{ct} exhibits the kinetics of interfacial electron exchange between the biofilm and the electrode surface and is strongly influenced by surface chemistry, biofilm conductivity, and electrode material. R_{diff} is reflected by the concentration gradients and mass transport limitations within biofilms and porous electrodes and could be determined by the Warburg region in EIS spectra. The R_{Ω} corresponds to the bulk resistance of the electrolyte and membrane and is proportional to ionic conductivity and interelectrode spacing. Miller et al. [133] studied the distribution of internal resistance within MECs to optimize design and operational conditions through analyzing single-chamber MECs with carbon cloth electrodes. The overall internal resistance analysis of components showed resistance by around 210 $\Omega{\cdot}cm^2$ for the anode, 77 $\Omega{\cdot}cm^2$ for the cathode, and 11 $\Omega{\cdot}cm^2$ for the solution. Moreover, it was realized that reducing electrode spacing had insignificant impact on the performance, however, it was declared that fluid motion between electrodes substantially lowered the resistance across all components with the anode resistance decreasing to 150 $\Omega{\cdot}cm^2$. Furthermore, by optimizing the anode-to-cathode surface area ratio to balance internal resistance, they found that increasing the ratio of anode to cathode has significant effect on improving the current density of MEC (Fig. 6a) leading to current density of 47 A/m^2 and a hydrogen production rate of 3.7 L-H_2/L/day. Cario et al. [134] introduced the Electrode Potential Slope method for evaluating internal resistance components in MECs by focusing on anode, cathode, and solution contributions. By employing carbon felt anodes in acetate-fed MECs, they recognized that the anode contributes to 59 % of the total internal resistance which was calculated at 71 ± 5 $m\Omega{\cdot}m^2$ primarily due to mass transfer limitations and substrate availability in stagnant fluid conditions.

It is important to remind that when comparing the resistance of anode electrode, the reactor configuration should be considered as an important parameter not only from geometrical aspect, but most importantly, for scenarios whether the reactor is membraneless or double chamber. For instance, in the above-mentioned studies Miller et al. used a single chamber MEC which allows direct ionic diffusion between the anode and cathode that could minimizes ohmic losses converse to Cario et al. that utilized a proton exchange membrane in dual-chamber MEC that led to additional ionic resistance and increases overall internal resistance. This is an important point from a system-level viewpoint, as the relative contribution of anode resistance to total cell resistance could appears lower/higher in a scenario, not necessarily due to improved anode performance but because of the addition or lack of resistive elements associated with a membrane.

In an important study, Rago et al. [135] analyzed the effects of external resistance on bioanode performance in MECs derived from an anode electrode taken from MFCs. By using different resistances (12, 220, and 1000 Ω) during the operation of the MFC, they found that low resistance (12 Ω) bioanodes supported higher *Geobacter* abundance and promoted better exoelectrogenic activity. When these bioanodes were transitioned to MECs, the 12 Ω anode showed the shortest startup time and highest hydrogen production by hitting the value of 1.54 L H_2/L/day which surpassed both of the 220 Ω and 1000 Ω configurations. Quantitative PCR confirmed a greater concentration of *Geobacter* in the lower-resistance biofilm. Indeed, their results showed the correlation of external resistance with enhanced current generation in which at applied voltage 0.8 V, the highest current intensities of 7.7, 6.3 and 4.5 mA were obtained by MEC_{12}, MEC_{220}, MEC_{1000} respectively, which exhibited the 41 % lower current for MEC_{1000} than MEC_{12}.

4.2. 3D anodes

In an interesting study, Baş et al. [136] investigated the performance of novel 3D-printed anode electrodes for MECs using feta cheese wastewater (FCW), cheddar cheese wastewater (CCW) and salted cheese wastewater (SCW) as the electrolyte. The study focused on the impact of various spiral geometries (rod, 1-cycled, 2-cycled, 3-cycled and 4-cycled spirals) printed with copper-based Electrifi filament (Fig. 7a) with respect to different wastewaters. Through various electrochemical analysis such as the CV, the EIS and the LSV, it was determined that the 1-cycled spiral anode demonstrated superior current density in electrochemical analysis and lower resistance, with hydrogen production rates five times greater than other configurations. Electrochemical analyses confirmed that spiral designs enhanced electrode-electrolyte contact which improved charge transfer. The electrochemical analysis

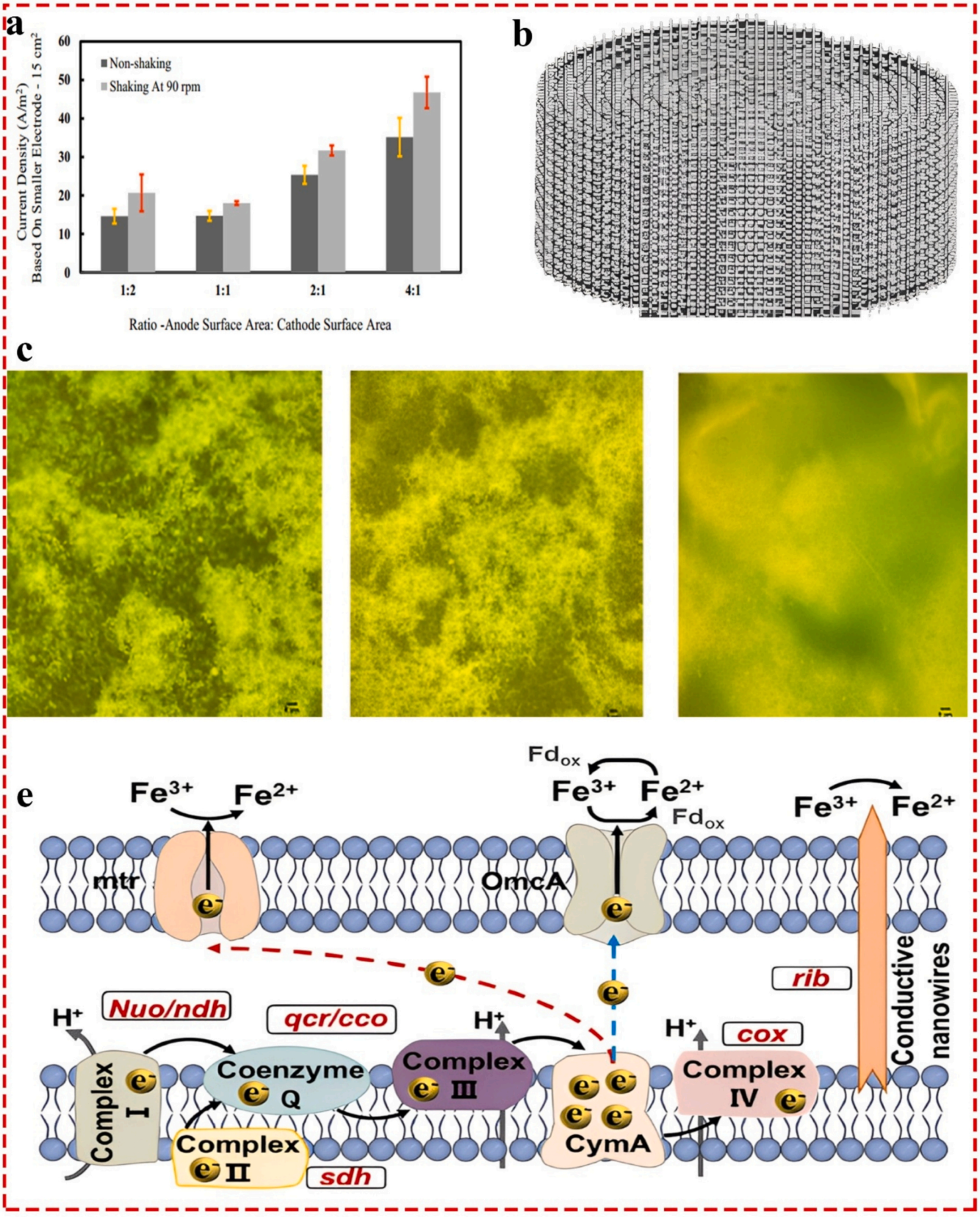

Fig. 6. a) Current density with various anode: cathode surface area ratios [133] reprinted with permission from Elsevier. b) 3D pictorial view of printed SS316 anode via laser melting [139] reprinted with permission from Elsevier. c) The formed biofilm on the surface Al-based alloy SS-316 PPy modified anodes [139]. d) Impact of Fe second anode on the electron production and transport (NADH dehydrogenase, c-type cytochromes, and riboflavin synthesis) [141] reprinted with permission from Elsevier.

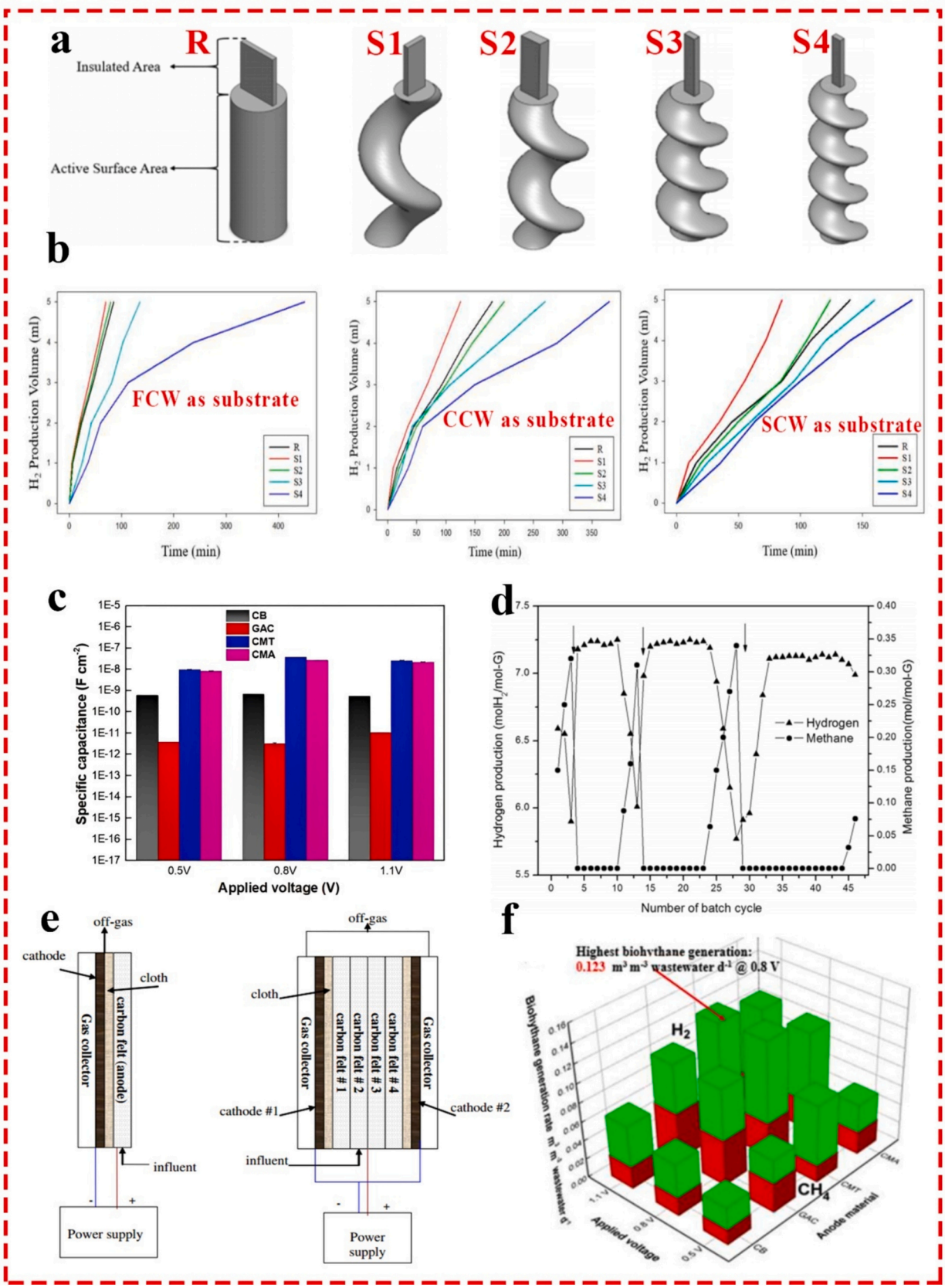

Fig. 7. a) 3D designed electrodes from left to right in order: Rod, 1-cycled, 2-cycled 3-cycled and 4-cycled spiral respectively [136] reprinted with permission from Elsevier. b) The time needed to generate 10 mL of hydrogen with different 3D electrodes with different electrolytes [136]. c) Specific capacitance derived from CV analysis [138] reprinted with permission from Elsevier. d) Variations of H_2 and CH_4 production with the number of cycle (the arrows represent the successive chloroform dosage: 3 %, 5 %, and 7 %) [146] reprinted with permission from Elsevier. e) Configurations of single anode–single cathode and multi-anode–multi cathode [144]. f) Biohythane generation rate ($m^3\ m^{-3}$ wastewater day^{-1}, green bar: H_2; red bar: CH_4) [138].

was further validated with examining the time needed to generate 5 mL hydrogen for all designed electrodes as well as three electrolytes. The findings revealed that the S1 is the fastest electrode in producing 5 mL hydrogen while the time needed to accumulate the hydrogen in FCS, CCW and SCW was about 70 min, 85 min, and 120 min correspondingly, indicating the FCW as the best electrolyte compare to the two others (Fig. 7b).

Lacroix et al. [137] implemented a multiphysics model to assess the performance of 3D bioanodes in MECs using domestic wastewater (dWW). The authors modeled various 3D graphite bioanode configurations and highlighted that a 20 mm thick bioanode optimizes current generation and COD removal around 86 % improvement over conventional electrodes. Moreover, beyond 20 mm thickness, the anode performance stagnates due to increased ohmic drop. Furthermore, the simulations revealed that stacking three 5 mm bioanode plates enhances convective transport and elevates current by 20 % yielded 33.5 mA and a COD removal of 61 %. Interestingly, by introducing a second cathode compartment the systems further raises current to 39.5 mA and achieved a 72 % COD removal.

Luo et al. [138] introduced a 3D-weaven anode network to improve biohythane (mix of hydrogen and methane) generation and nitrogen recovery in MECs through four scenarios of using carbon mesh (CB), granular activated carbon (GAC) and two carbon mesh electrodes with vertically and horizontally extended geometries namely CMA and CMT respectively. They demonstrated that this novel structure (The horizontally-extended carbon mesh denoted as CMT) can achieve a high biohythane production rate of 0.123 m^3/m^3 of treated wastewater daily at 0.8 V (Fig. 7f), with energy consumption of nitrogen recovery reduced to 0.77 kWh/kg.N which was substantially lower than traditional methods requiring over 1 kWh/kg.N. Moreover, they performed specific capacitance analysis as an effective indicator to directly elucidate the electrogenic activity of the electrode and microbe-electrode interaction which exhibited that the CMA and CMT reactor at 0.8 V had substantially higher specific capacitance at 2.61×10^{-8} and 3.64×10^{-8} F. cm^{-2}, correspondingly, than those of GAC and CB at 3.12×10^{-12} and 6.65×10^{-10} F.cm^{-2} (Fig. 7c).

In another study [139] Kumar and co-workers employed 3D printing to fabricate a stainless-steel anode which modified by polypyrrole to increase the hydrogen production in a membraneless MEC. The anode was fabricated through using laser melting to prepare two types of metal-based anode from stainless steel 316 and aluminium alloy in a spiral shape and with controlled porosity (Fig. 6b). The inverted fluorescence images exhibited a highly dense of biofilm formation on modified-PPs SS316 anode compared to the Al-based anode (Fig. 6c) results in hydrogen production by around 2.89 and 1.69 m^3/m^3/day respectively, which highlighted 71 % improvement in H2 production. This significant improvement not only highlighted the role of 3D printed electrodes, but it brought the exceptional effect of using conductive polymers in improving anode electrodes. However, it should be reminded that, aluminium and SS316 have different corrosion resistance which was not discussed by the authors. This is particularly important for long-term operations studies, as SS316 is highly resistance alloy compared to its counterparts. Indeed, in comparative analysis where two different materials are comparing factors such as corrosion, cost of materials and life cycle assessments are important aspects for translating a lab-scale technology to real world applications [140].

It is important to point out that, a 3D electrode augments the EET and mass transport by increasing the accessible electroactive surface area, reducing local diffusion paths, and improving flow and biofilm distribution within the electrode. Furthermore, spiral geometry yields a large geometric and volumetric surface area per volume of reactor while it would limit the local current density hotspots for a more uniform biofilm colonization. These features previously demonstrated that, how increasing electroactive area boost current densities between 3.4 and 12 times higher compared to pristine anodes [130,131], due to the higher number of accessible sites for microorganisms, shorter diffusion distance and lower ohmic drops throughout the electrodes.

4.3. Acclimation procedure

Li et al. [142] investigated the influence of various anode acclimation strategies on MECs using various feedstocks, including corn stalk fermentation effluent (CSFE), along with acetate, butyrate and reported the butyrate-acclimated anodes as boosters of microbial electroactivity and substrate utilization. The configuration showed significant improvements in VFA degradation, particularly in butyrate removal which reached 62 % compared to much lower rates in the acetate and CSFE feedstocks. Electrochemical analysis indicated superior electron discharge capabilities in butyrate-acclimated anodes with optimal biofilm development, high current generation and coulombic efficiency. The findings exhibited that the butyrate-acclimated MEC attained superior hydrogen production rate of 4.52 m^3 H_2/m^3/d. In another study, Ullery et al. [143] analyzed the impact of different anode acclimation methods and reactor configurations in MECs for treating cellulose fermentation effluent. They compared mini MECs with cube MECs and find that pre-acclimation with domestic WW enhances COD removal, with mini MECs achieved slightly better removal rates (up to 86 %) than cube MECs (82 %). Protein removal efficiency also increased, with mini MECs and achieved to 84 % removal in domestic WW-acclimated systems. Interestingly, the results highlighted the insignificant differences of hydrogen recovery between two configurations. Moreover, current densities were consistent across both reactor types, while COD removal was influenced by pre-acclimation, which suggested a biofilm enriched with a diverse microbial community can significantly improve treatment efficiency in MECs toward handling complex waste streams.

4.4. Anode arrangement

Gil-Carrera et al. [144] examined the optimization of anode-cathode configurations in MECs to enhance hydrogen production by focusing on anode arrangement in two configurations named single-anode/single-cathode and multi anode-cathode (4-anodes and two-cathodes) (Fig. 7e) considering anode thickness and cathode placement. By utilizing multi-layer carbon felt anodes and gas diffusion cathodes in a single chamber flat-plate MEC setup, they observed that increasing the anode from a single layer to two layers of 5 mm thickness improves hydrogen production up to 245 mL/day under optimal conditions. Moreover, the impact of cathode configuration was also examined, and it was revealed that adding a second cathode increases current output but leads to higher methane production due to hydrogenotrophic activity. Protein analysis indicated greater microbial density on anodes closest to the cathode which supported the influence of spatial arrangements on microbial growth. It is worth noting that the spatial arrangement has a direct impact on pH gradients, nutrient flux, and hydrogenotrophic microbial activity. This effect occurs through regulating ions transport and gas diffusion paths. Indeed, it means that when the distance between anode and cathode become shorter it led to diminish ionic paths as well as ohmic loses, while at the same time, it also improves proton flux toward cathode. On the other side of the coin, when the distance between anode and cathode is larger, it could lead to microenvironment changes by acidifying anode microenvironment due to proton accumulation and alkalizing the electrolyte in vicinity of cathode due to hydroxide generation. Collectively, these chain reactions result in lower buffer capacity and suppression of hydrogenotrophic methanogens.

Liang et al. [145] demonstrated that optimizing anode arrangements in MECs significantly improves system efficiency. They arranged graphite felt anodes on opposite sides of the cathode in a stacking configuration and achieved a substantial reduction in solution, polarization, and biofilm resistances, which was confirmed by the EIS analysis. The modified design resulted in a 72 % increase in current density and a 118 % increase in hydrogen production rate by about 5.56 m^3 H_2/m^3/

day at a 0.8 V applied voltage. Moreover, it was found that the stacked anode design operates as a parallel circuit enhances anodic efficiency and effectively doubling cathode surface utilization. The setup achieved a maximum hydrogen rate of 10.88 m^3 H_2/m^3/day at 1.5 V which highlighted the potential of electrode arrangement optimization as an economical strategy for scalable MEC applications. Zhang et al. [146] investigated the impact of a double anode arrangement in MECs on hydrogen production from glucose while employed chloroform as a methane inhibitor to enhance efficiency. Importantly, the EIS and the CV analysis confirmed that electron transfer primarily occurred via biofilm-bound redox compounds rather than soluble shuttles which highlighted the strong biofilm activity on the anodes. Moreover, through adding 5 % (v/v) chloroform, methanogenesis was inhibited after the third cycle and completely suppressed across the rest of batch cycles that enabled continuous hydrogen production without methane byproducts (Fig. 7d) in which the setup achieved a maximum hydrogen rate of 2.39 m^3 H_2/m^3/day. Additionally, energy efficiency relative to electrical input reached 165 % demonstrated the double anode's potential for enhanced biohydrogen yield and substrate utilization. Indeed, these results emphasized that the combined benefits of an optimized anode structure and methanogen suppression in improving MEC performance. Li et al. [147] integrated dark fermentation with a single-chamber MEC, which utilized by double anode arrangement to enhances biohydrogen production from corn stalk. Their findings exhibited that a hydrogen production rate of 3.43 m^3 H_2/m^3/day in the MEC stage with an applied voltage of 0.8 V effectively doubling the bio—H_2 yield compared to standalone dark fermentation. Importantly, their findings showed that the dual-anode setup improved current density and coulombic efficiency by around 340 A/m^3 and 71 % respectively. Electrochemical analyses revealed that VFAs, such as acetate were major electron donors, leading to 90 % conversion of acetate to bio-H_2 and 44 % COD removal. In an interesting study, Guo and colleagues [141] proposed to use iron as a second anode alongside a graphite brush to improve biohydrogen production and phosphorus recovery. The authors stated that by adding the second iron anode the EET significantly would be improved through ferrous ion contribution. Indeed, the synergies of double carbon/iron anodes results in the electrode efficiently benefiting from all EET mechanisms (i.e., direct, soluble and matrix) as electrons are moving to protein complexes I/II on the cell membrane, thereafter, crossing cytochromes to protein complex III and finally to complex IV. On the other hand, electrons from inner membrane's c-type cytochromes would move to electron carrier proteins on the outer membrane (such as MtrABC and OmcA), which then drive the dissimilatory iron-reducing bacteria (DIRB) to carry out the iron reduction process (Fig. 6e). Their findings revealed that adding iron as the second anode results in extraordinary improvement of more than 8 times in terms of hydrogen production and COD removal in MEC. Although using stacked anode has several advantages such as reaching to higher current densities and stability it also contributes to trade-offs that has adverse effect on MEC performance. One the main problem is the unbalanced potential distribution throughout stack because of increasing the ohmic resistance as the result of increasing current path length and interelectrode space. This problematic issue brings another fact into the spotlight which is the nonuniform biofilm development that led to utilizing electrons within layers unevenly. Additionally, limited the convective flow could lead to constrains on substate diffusion, pH microenvironment changes which altogether led to reduce the rate of EET. Last but not least, stack anodes could suffer from hydrogen and carbon dioxide accumulations between stacked layer which can adversely impact the rate of biohydrogen production.

4.5. Electrodes ratio and spacing

The effect of the electrode ratio can be analyzed from two avenues. The first one is the ratio of the anode electrode to the cathode, and the second one is the ratio of the anode electrode to the anode chamber. Baek et al. [148] evaluated the effect of varying electrode size ratios (Fig. 8a) on internal resistance and current densities in MECs. Through utilizing polarization data, the authors observed that equal cathode-to-anode ratios (1:1) generated the highest current at 1.8 mA with an applied voltage of 0.9 V, while reducing anode size led to limiting currents around 0.8–1.0 mA at lower applied voltage. Moreover, they found that larger anodes minimize total resistance, which contributed in 57 % of internal resistance in smaller configurations. Interestingly, it was realized that by adjusting electrode size the biogas composition also was impacted, where the setups with lower ratios favoured hydrogen, in contrast to higher ratios which results in more methane production. However, the highest hydrogen recovery rate of by around165% was obtained at a 1:1 ratio (Fig. 8c). Interestingly, Wang and co-workers [149] in another study found that a stacked high surface area ratio of anode to cathode results in superior hydrogen production in membraneless MEC. They used a single chamber MEC bioreactor with 644 mL capacity and working volume of 500 mL with stacked anode with effective area of 160 m^2/m^3. Their findings revealed that the MEC generated hydrogen at the rate of 39.8 ± 1.9 L/L/D with limited rate of methane production due to the use of methanogenesis inhibitor. It should be noted that the reactor size, the rate of substrate, geometry have significant effects on the effect of ratio on the production performance of MEC. Guo et al. [150] investigated the effect of the cathode-to-anode surface area ratios on methane production in MECs using artificial beer wastewater as medium. By testing three configurations ratios (ratios of 1, 2.5, and 4 cm^2/cm^3) they found that increasing the ratio significantly enhanced methane yields and energy efficiency. At a cathode-to-anode ratio of 4 cm^2/cm^3 and an applied voltage of 0.9 V methane production reached 0.14 m^3 CH_4/m^3/day leading to 1.8-fold improvement over the lowest (1 cm^2/cm^3) ratio setup. Moreover, the COD removal rates were consistent across configurations and suggested that cathode area impacts methane output rather than substrate degradation. Electron balance analysis indicated a greater proportion of electrons contributing to methane generation as the cathode surface area increased which highlighted the role of cathode size in enhancing electrochemical and microbial contributions to methane recovery in MECs. Cheng and Logan [151] examined the effect of distance between the anode and cathode electrodes from 1 to 3.5 cm on the performance of MEC in a wide range of applied voltage. The results indicated that electrode spacing is not mutually exclusive with applied voltage where the highest hydrogen produced at an applied voltage of higher than the 0.6 V, however, at lower voltage the electrode space of 1 cm results in higher H_2 generation (Fig. 8b). Their results indicated the hidden relation and interaction between applied voltage and electrode space which is critical when the aim is to optimize the electrode space with respect to applied voltage and vice versa. In an interesting study, Fonseca and coworkers. [152] realized how the ratio of filling the anode chamber by carbon electrode could impact the acclimation process and total yield of biohydrogen production. The performance of MEC evaluated under three different scenarios when the graphite brush diameters were 1.5 cm, 4.5 cm and 5.5 cm (Fig. 8d) considering the chamber's diameter at 5.5 cm. The findings exhibited that when the chamber was completely filled (for 5.5 cm), maximum current and total hydrogen production were obtained compared to two other scenarios (Fig. 8f). It should be noted that these results are for the case of graphite brush which could be experimented and validated for other carbon-based materials such carbon cloth and carbon felt that are extensively employed in MECs as the anode.

4.6. Encapsulation

Rozenfeld et al. [153] explored the use of a semi-single-chamber MEC incorporating an anode encapsulated in a dialysis bag to enhance hydrogen production and biofilm stability. By encapsulating carbon cloth and stainless steel (CCSS) anodes in dialysis bags with molecular weight cut-offs (MWCO) of 2, 14, and 50 kDa, they reduced non-

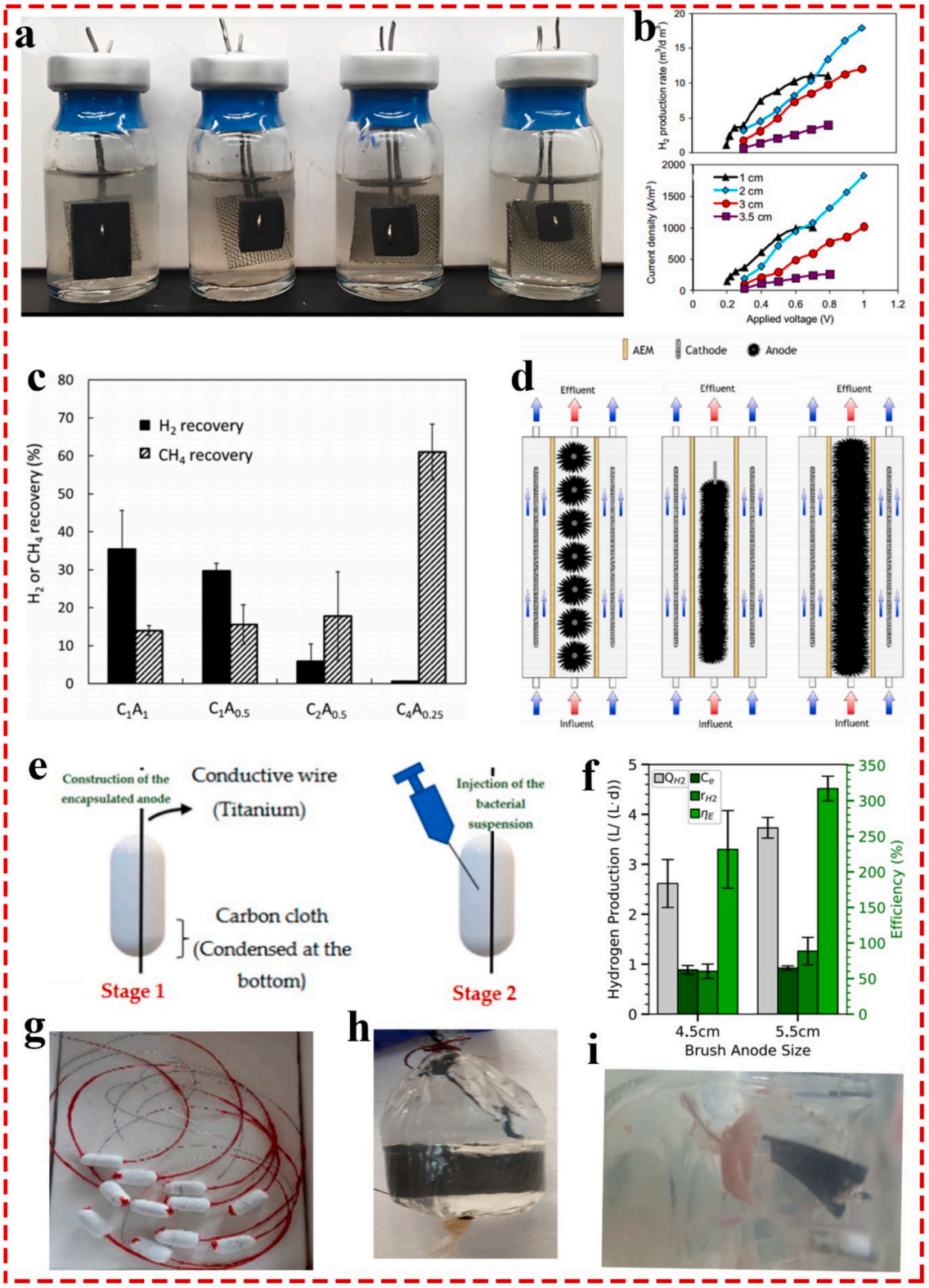

Fig. 8. a) Pictorial view of anode-cathode at different ratios [148] reprinted with permission from Elsevier. b) The rate of hydrogen production rate (top) and current density (bottom) as the function of applied voltage at different electrode distance [151] reprinted with permission from Elsevier. c) The variation of methane and hydrogen recovery efficiencies for the various electrode surface area ratios [148]. d) Sketch of graphite brushes with 1.5 cm, 4.5 cm, 5.5 cm diameter [152] reprinted with permission from Elsevier. e) Encapsulation anode preparation scheme [155] reprinted from open-source. f) The rate of Hydrogen generation (QH2) and efficiency analysis for the single graphite brush anode of Coulombic efficiency (Ce), overall hydrogen recovery (rH2), and the energy yield relative to electrical input (hE) [152] reprinted with permission from Elsevier. g) Actual photo of encapsulated anodes [155] reprinted from open-source. h and i) The encapsulated anode in the dialysis bag before inoculation and after insertion of the anode to the MEC chamber and inoculation with *G. sulfurreducens* respectively [153] reprinted with permission from Wiley.

exoelectrogenic bacterial invasion and improved *Geobacter sulfurreducens* biofilm formation. The D50- CCSS anode yielded the highest hydrogen evolution rate of 0.160 m^3/m^2/day which surpassing the non-encapsulated anode by 24 %. Current density also hit at 16.34 A/m^2 under 0.6 V, compared to 12.19 A/m^2 for non-encapsulated setups. This design demonstrated that the encapsulated anode approach effectively enhances MEC performance by sustaining bioelectroactivity, minimizing contamination and improving hydrogen output particularly in setups involving complex substrates like wastewater. Gandu et al. [154] assessed the impact of encapsulating *Geobacter* on carbon-cloth anodes using alginate and alginate-chitosan and compared the results in a scenario with a non-immobilized biofilm. The SEM images demonstrated a highly dense biofilm formation on the surface of the electrodes (Fig. 9d, e) compared to the control electrode (Fig. 9c). By comparing anodes with alginate-chitosan (AC) and only alginate (A) encapsulation against a non-immobilized setup, they found that in wastewater-fed MECs, the AC anode achieved the highest current density of 11.52 A/m^2 at 0.2 V, which was 29 % higher than the non-immobilized anode. The immobilized AC anode also provided superior hydrogen evolution rates by about 0.56 m^3 H_2/m^3/day along with a COD removal efficiency of 75 %. Additionally, the microbial diversity based on 16S rRNA for each anodic biofilm was evaluated and it was realized that the microbial diversity for both scenarios (A and AC) predominantly composed of *Geobacter sulfurreducens* (92 %) compare to the non-encapsulated anode (only 74 %) which explicitly highlighted that this strategy effectively excluded non-exoelectrogenic bacteria (Fig. 9a). Interestingly, Dubrovin et al. [155] constructed oval-shape anodes (Fig. 8g) and encapsulated pure-culture of *Geobacter sulfurreducens* (by injecting the microbial suspension within the capsules) with acetate and synthetic wastewater (SW) for 32 and 46 days respectively (Fig. 8e). The LSV analysis exhibited that the current density hits the 1.70 ± 0.22 A m^{-2} which was doubled compared to the control. Moreover, it was realized that the rate of biohydrogen production for the acetate-fed and SW-fed for encapsulated and control MEC reached to 0.027 and 0.017 m^3 m^{-3} day^{-1}, 0.006 and 0.005 m^3 m^{-3} day^{-1} respectively, leading to improvements by several fold.

In another study, Duboriabn et al. [156] compared the effect of encapsulated materials in dialysis bag as an anode in MEC. They compared three anodes which are encapsulated with graphite particles in dialysis bag, bare anode in bag and bare anode without a bag, The experiments were conducted based on the two mediums of synthetic wastewater and Geobacter as the medium and reported that the graphite based outperformed the two other anodes in terms of hydrogen production, COD removal, and current density. Moreover, the graphite-based encapsulated anode resulted in a higher electroactive bacteria population.

In an interesting analysis, Hirsch and co-workers [157], comprehensively evaluated the role of encapsulation on the effectiveness of carbon felt in four scenarios. Four anodes which are encapsulated carbon felt infilter bag, bare carbon with alginate hydrogel, encapsulated carbon felt alginate hydrogel (ECAH) and bare carbon as a control were examined (Fig. 10a). The findings indicated that the charge transfer resistance in the ECAH dramatically reduced leading to superior biohydrogen generation. Interestingly, the synergies of using a polymer and encapsulation resulted in an exceptional difference between bare anode and encapsulated alginate hydrogel anode where the percentage population of *Geobacter sulfurreducens* for modified electrode and the bare anode was examined by around 79 % and 3 % respectively.

Interestingly, encapsulation imposes a selective diffusive barrier between bulk liquid and immobilized cells that changes substrate and product fluxes leading to microorganisms' persistence within capsules. Indeed, encapsulant's pore structure and effective molecular-weight cutoff (MWCO) determine which solutes cross by diffusion where small metabolites and common redox mediators diffuse readily through soft hydrogels and larger proteins, enzymes or macromolecular flocs are excluded when the MWCO is below their molecular weight. Collectively, encapsulation can result in a rapid-diffusion of electroactive bacteria that rely on small soluble mediators while excluding large competitors or predators.

4.7. Utilizing nanomaterials

Chavan and Gaikwad [158] converted lignocellulose (*Bambusa bambos*) in series of reactions by successive enzymatic pretreatment through mixing with laccase to delignify biomass, followed by enzymatic hydrolysis by utilizing cellulose with the delignified biomass (Fig. 9f) and decorating with Fe nanoparticle on the anode electrode for highly efficient microbial electrolysis hydrogen production. Through enzymatic pretreatment, they achieved a 40.31 % reduction in lignin which allows for enhanced cellulose hydrolysis and resulting in a glucose yield of 99.54 mg/dL. Moreover, through decorating anode with Fe nanoparticles, the CV analysis demonstrated superior electrochemical performance for Fe coated anode compare to non-coated electrode (Fig. 9g) where at applied voltage of 0.8 V the rate of hydrogen production increased by 1.14 times compared to uncoated setups and reached to a peak production of 0.02 g H_2 per gram of biomass (224 mL/g). What's more, coating the Fe nanoparticles improved biofilm formation and extracellular electron transfer due to increased surface roughness and biocompatibility which was proved by enhanced current density in the CV analysis. Zakaria et al. [159] assessed the impact of silver nanoparticles (AgNPs) on the electrocatalytic activity and microbial community composition of an anode biofilm. The study exposed a *Geobacter*-enriched biofilm to 50 mg/L of AgNPs and found that the current density remained stable at 14.2 A/m^2 despite of AgNP exposure. The SEM images exhibited that AgNPs accumulated within the biofilm matrix without penetrating bacterial cells while EPS production increased which significantly providing a protective barrier against AgNP toxicity (Fig. 11c, d). Post-exposure analysis revealed a 28 % increase in *Geobacter* abundance, while other bacteria, such as *Acinetobacter* and *Dysgonomonas*, declined which probably indicating the selective tolerance (Fig. 11e). These findings highlighted the resilience of *Geobacter*-dominated biofilms under AgNP stress, suggesting the potential for MECs to operate effectively in environments with antimicrobial nanoparticle contaminants. San-Martín et al. [160] explored the degradation of 2-mercaptobenzothiazole (MBT) in microbial electrolysis cells with graphene-modified anodes to enhance microbial community diversity and reduce biotoxicity. They identified five primary degradation pathways and two dimerization routes for MBT with graphene-modified anodes promoting advanced degradation through hydroxyl radical reactions. These electrodes reduced MBT toxicity from 46.2 to 27.9 eqtox•m^{-3} compared to minimal reductions in unmodified setups. Microbial analysis showed an enrichment of *Geobacter* and *Bacteroides* on the graphene anodes, along with *Rhodococcus*, which contributed to further hydroxylation of MBT. Furthermore, graphene modifications resulted in increased current output and more effective COD removal which exhibited that electrode surface modification can both enhance pollutant degradation and foster particular microbial communities capable of managing complex contaminants. Xu et al. [161] investigated the use of iron nanoparticle-decorated graphite anodes (Fig. 9b) to enhance current density and biofilm formation in MECs with *Shewanella oneidensis MR-1*. The Fe-decorated anodes achieved a maximum current density of 42.5 μA/cm^2 which was 8.25 times higher than plain graphite anodes. Moreover, the whole genome microarray analysis revealed that genes involved in biofilm formation, such as flagellum and type IV pilus-related genes were upregulated which indicated stronger microbial attachment. Additionally, genes associated with electron transport, including c-type cytochromes and flavins, showed increasing expression and facilitating enhanced electron transfer from bacteria to the anode in Fe decorated anode. The study emphasized the role of nanoparticle-modified surfaces in promoting biofilm stability and boosting MEC performance by augmenting microbial electroactivity and electron transport mechanisms.

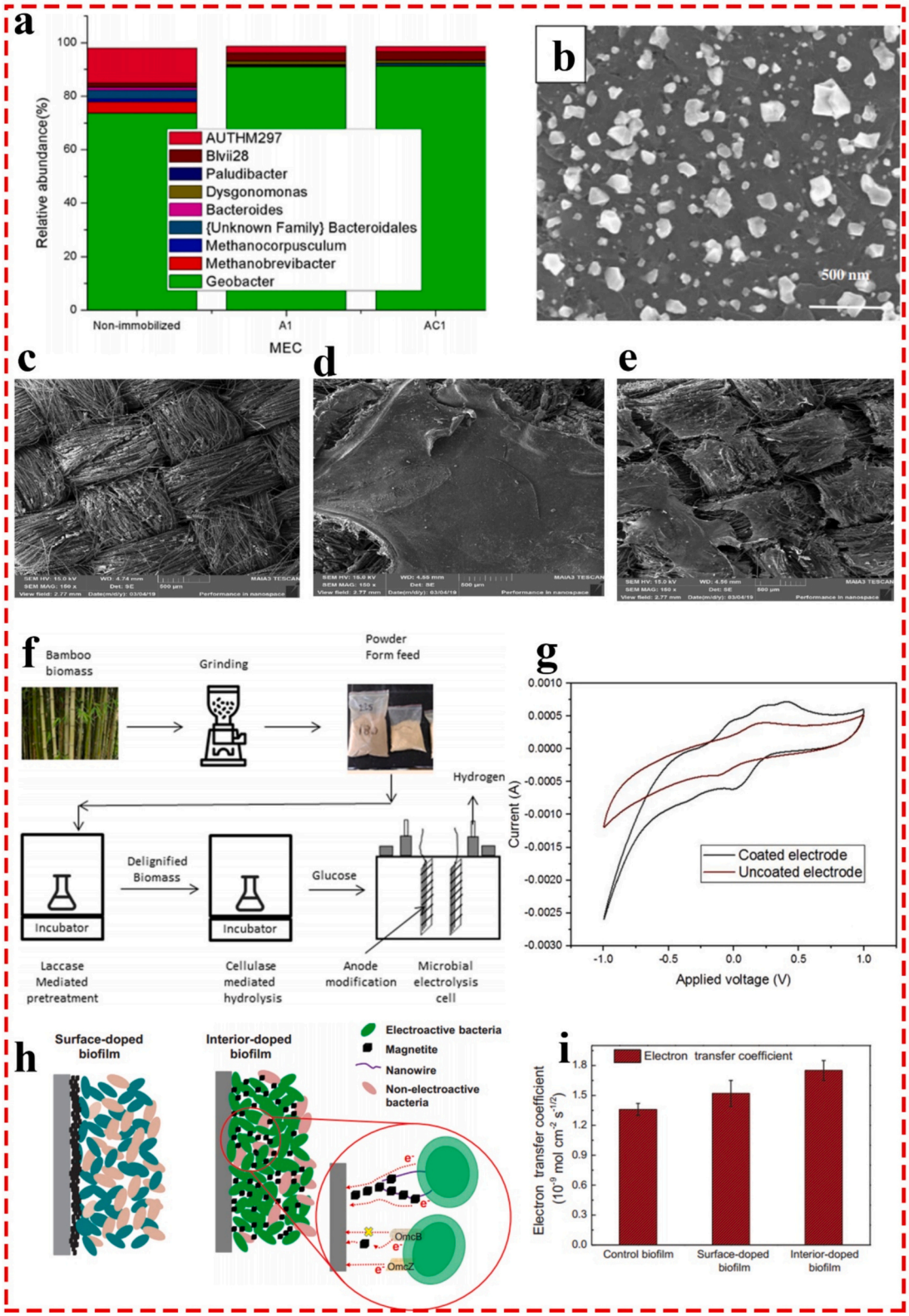

Fig. 9. a) Microbial diversity analysis with respect to genus for alginate (A1), alginate-chitosan (AC1) and control biofilm [154] reprinted with permission from Elsevier. b) The SEM image of Fe nanoparticle decoration on the graphite electrode [161] reprinted with permission from Springer. c, d and e) The SEM images of Control biofilm, alginate (A1) encapsulated and alginate-chitosan (AC1) respectively [154]. f) Schematic representation of the multiple steps involved in *Bambusa bambos* conversion to hydrogen by successive enzymatic treatment and microbial electrolysis [158] reprinted with permission from Elsevier. g) The cyclic voltammetry analysis for Fe coated and uncoated anode [158]. h) Surface coated and interior doped of magnetite nanoparticles in anode electrode [162] i) The electron transfer coefficient of surface coated, interior doped of magnetite and control systems [162] reprinted with permission from Elsevier.

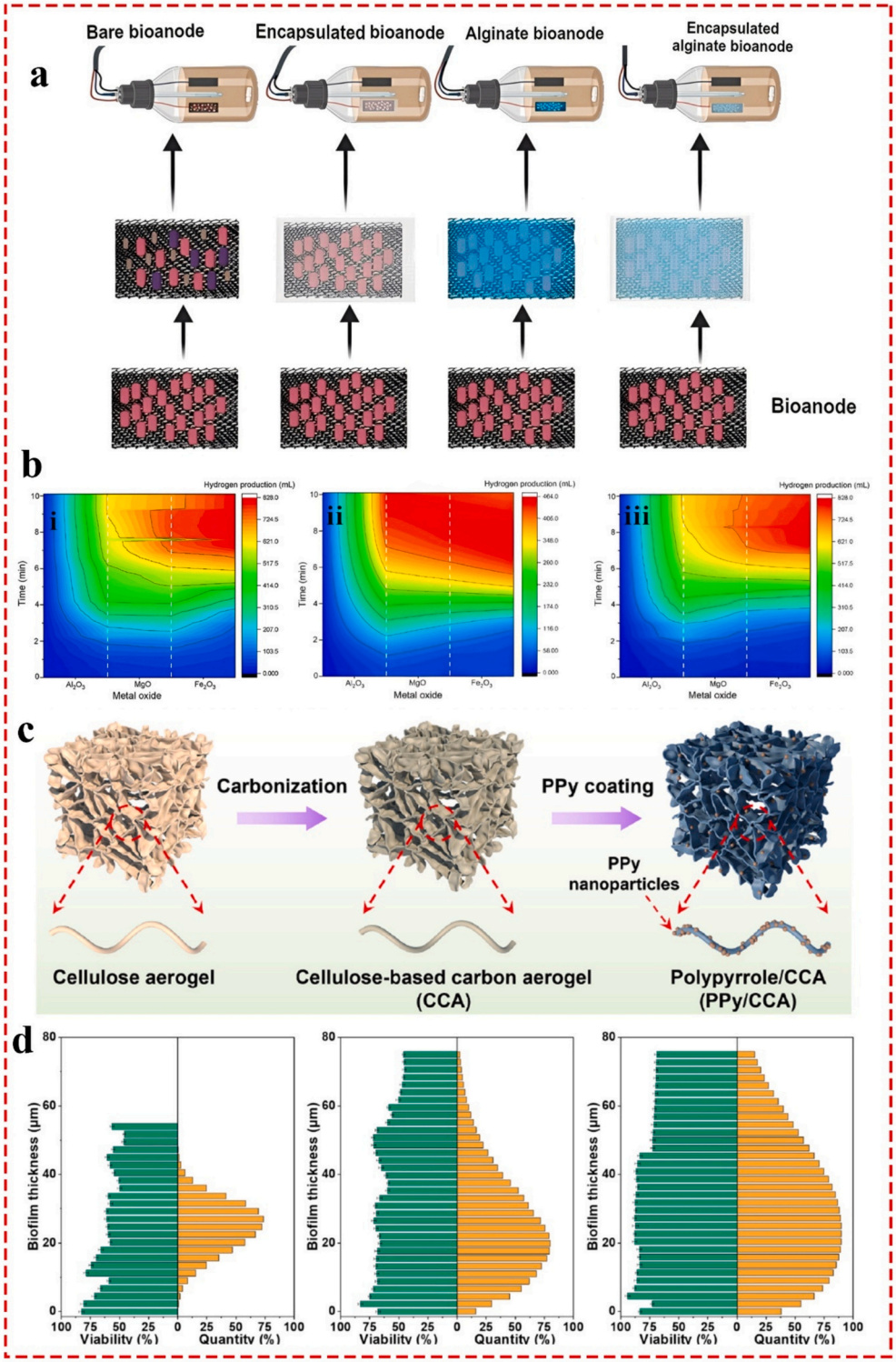

Fig. 10. a). Bioanodes (pre-acclimated bioanodes with *G. sulfurreducens*). Bare bioanode (without any modification), encapsulated bioanode (bioanode inserted into a filter bag), alginate bioanode (bioanode immersed with alginate), and encapsulated alginate bioanode (bioanode immersed with alginate and inserted into a filter bag) [157] reprinted from open-source. b) The rate of hydrogen production using different metal oxide materials at various dosages of 0.5 g (i), 1 g (ii), and 2 g (iii). [165] reprinted with permission from Elsevier. c) Preparation process of cellulose-based aerogel PPy anode. [166] d) bacterial viability and quantity along the thickness of biofilms formed on graphite (left), cellulose-based aerogel (center), and cellulose-based aerogel PPy (right). [166] reprinted with permission from Elsevier.

Interestingly, surface-decorated Fe nanoparticles and iron oxides not only catalyze redox cycling (Fe^{3+}/Fe^{2+}) and improve heterogeneous electron exchange between electrode and mediators or cells, but it boosts surface roughness and polar groups that augment microbial adhesion and dense electroactive biofilms. Moreover, Fe^{3+} additions modify metabolism of iron-reduction coupled VFA oxidation and accelerates VFA degradation kinetics, while magnetite can stimulate direct interspecies electron transfer and functionally complement or promote

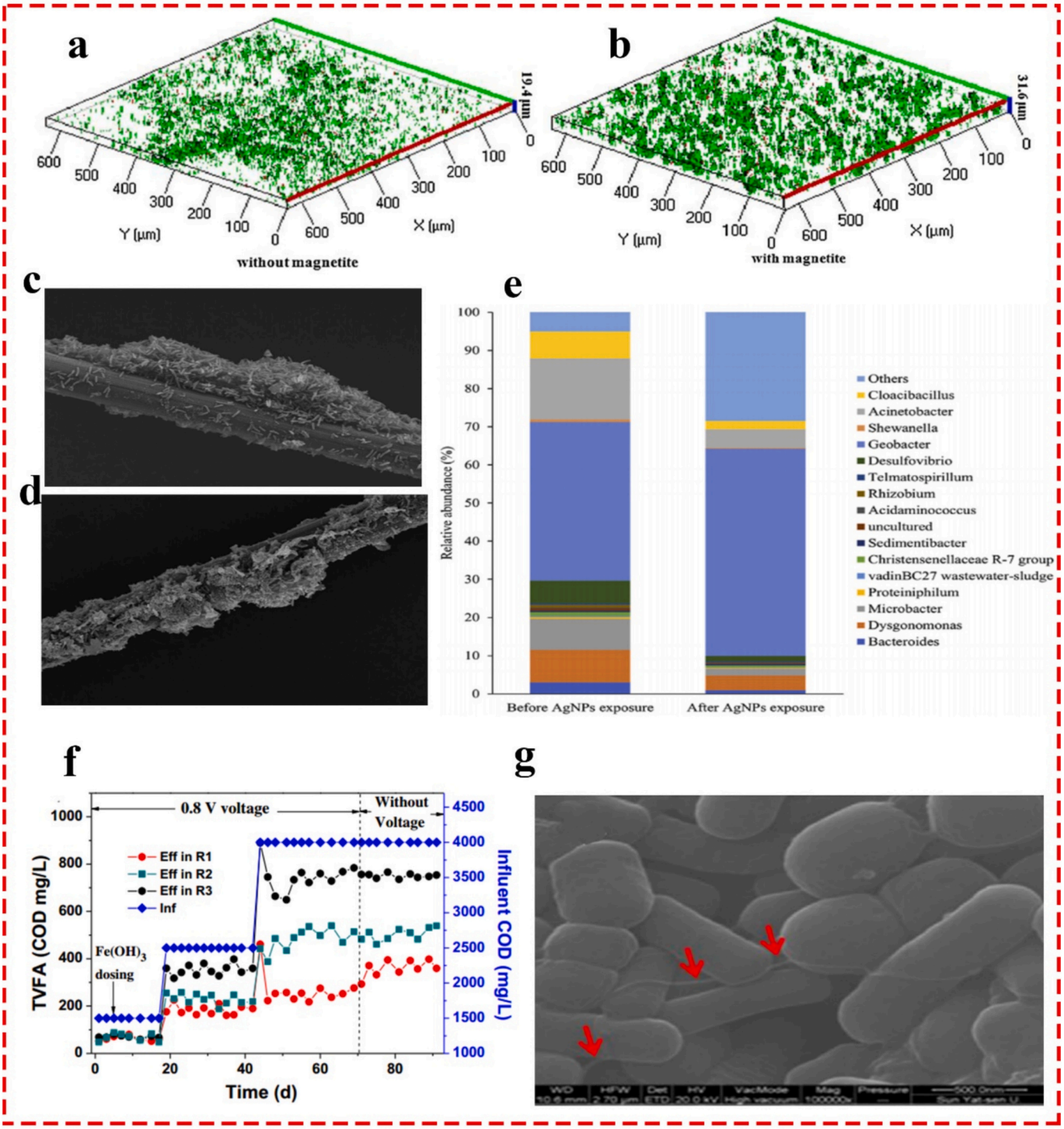

Fig. 11. a and b) Accumulation thickness of biofilm on the surface of electrode without and with Fe3O4 correspondingly [164] reprinted with permission from Elsevier. c and d) The SEM images of anode biofilm before AgNPs exposure and anode biofilm after AgNPs exposure respectively [159] reprinted with permission from Elsevier. e) Relative abundance of bacterial communities at genus levels [159] reprinted with permission from Elsevier. f) Effluent TVFA concentrations in the three reactors (R1, R2 and R3) [163]. g) The SEM image of the surface in SRB-biocathode with magnetite addition [164] reprinted with permission from Elsevier.

conductive-pili mediated electron transfer in mixed communities.

As can be observed, Fe is an important additive element to boost the performance of microbial electrochemical systems like MECs. In this regard, Zhang et al. [163] added Fe(III) to a single anaerobic digestion (AD) in an integrated MEC-AD system to understand the effect of the Fe additive on the COD removal and microbial diversity. Through the findings, they reported superior rate for degrading organics via augmenting anaerobic degradation ability of VFAs under dissimilatory Fe (III)-reducing conditions. Moreover, the reduced Fe(II) from Fe(III) reducing process together with the electric field led to more EPS production which was favorable for the enrichment of bacteria in the anode biofilm. Hu et al. [164] investigated the effect of magnetite nanoparticles on enhancing sulfate reduction in MECs utilized by biocathode. By incorporating 0.64 mM magnetite into the biocathode, 122 % increase in sulfate reduction rate achieved (around 152 g/m^3/day) in comparison to the control. The presence of magnetite doubled peak

current density in CV tests, which indicates enhanced electrochemical activity. The SEM images (Fig. 11g) revealed that magnetite nanoparticle promoted the formation of conductive pili-like structures and iron-sulfide deposits within the biofilm which facilitated electron transfer where the thickness of the biofilm increased from 19.4 μm to 31.6 μm with and without Fe_3O_4, respectively (Fig. 11a, b) and lead to an improvement of around 62.8 %. Additionally, magnetite increased the relative abundance of *Desulfovibrio* species from 27.5 % to 72.2 %, which correlated with an improved electron recovery efficiency rising from 29.6 % to 56.1 %.

Although the focus of this review is on the anode electrodes in MECs, it is worth mentioning similar strategies for the anode electrode in MFCs were adopted too, as anode in both systems has almost similar condition. In an interesting study, Liu et al. [162] evaluated the effect of employing different strategies on decorating magnetite nanoparticles on anodes of MFCs through two scenarios. In the first one, nanoparticles were coated on the surface of the anode electrode while in the second scenario, it implanted within the formed biofilm (Fig. 11h). The findings revealed that the interior-doped Fe nanoparticle generates higher rate of electron transfer than surface-coated and controlled electrode (Fig. 11i). This highlighted the significance of selecting an appropriate strategy on applying a method with two different approaches which could leading to different results. The electron percolation network in magnetite-assisted anodes is highly influenced by the adopted strategy that whether consider is doping or surface coating. Generally, through coating provide a conductive layer on the electrode surface that bridges microbial redox sites and the carbon substrate and provide rapid charge transport pathways. On the other hand, doping magnetite incorporation embedded conductive Fe3O4 domains throughout the carbon framework and create continuous electron-conducting channels that lowers charge-transfer resistance (R_ct) more effectively by increasing volumetric conductivity, while coatings primarily reduce interfacial resistance.

In another study, Goren et al. [165] evaluated the effect of adding various nanomaterials in MECs to improve the EET process and the rate of biohydrogen production. Three nanoparticles including Al2O3, Fe2O3 and MgO at three dosages (0.5 g, 1 g, 2 g) were used to find the optimum fraction and best nanoparticle compared to the control group accordingly. The findings revealed that at the dosage 0.5 g, hydrogen production reached 448 mL, 455 mL, 464 mL for Al_2O_3, MgO, and Fe_2O_3 respectively, compared to control 442 mL. Increasing the dosage of nanomaterials to 1 g results in maximum production of hydrogen for all nanomaterials with Fe_2O_3 obtained the highest almost twice as the controlled around 827 mL. This is probably due to the strengthening of the ionic solution and increasing the metabolic activity of microorganisms leading to superior EET (Fig. 10b). However, increasing to 2 g led to a marginal reduction on productivity due to the toxicity of nanoparticles to electroactive bacteria.

Wang et al. [167] compared two anodes performance on single-chamber microbial electrolysis cells which are three layered carbon cloth anode and the nitrogen-doped CNT and reported higher hydrogen production and biofilm activity for the N-doped CNT compared to the layered anode due to structural changes, promoting functional groups and increasing hydrophilicity of the anode. Interestingly, this study also highlighted the significance of implementing an advanced nanostructured functional materials strategy over physical strategy.

4.8. Utilizing polymers

Coating polymers significantly improve charge transfer and conductivity through regulating microbial EET and biofilm adhesion. Indeed, conductive polymer such as polyaniline (PANI), polypyrrole (PPy), and PEDOT/PSS facilitate rapid electron transport at the interface of biofilm and electrode and reduce charge transfer resistance. Conductive polymers by introducing positive charges on electrode surface attract negative charge bacteria (which typically are electroactive microorganisms) with more strong bonding and form a dense biofilm. In this regard, utilizing different conductive polymers is suggested as a facile and low-cost strategy to improve anode/cathode performance and microbial communities [168,169]. For instance, Seelajaroen et al. [170] used chitosan to augment the EET process of anode in MEC to increase the rate of biomethane production. In another study, Rahmadita and colleagues [171], coated a thin layer of polyaniline on anode in a single chamber MEC to improve the reduction rate of ammonia contents in liquid waste fertilizer wastewater and reported the performance of MEC in ammonia is doubled while on the other hand the design consortium was capable of adapting and surviving in high ammonia environment. In another study, Guo and co-workers [172] compared the effect of coating polypyrrole on the surface of carbon electrode and study its impact on the rate of electron transfer and removal of NO through denitrification process in a dual chamber MEC. The results demonstrated that polymer modification results in more than 25 days of stable operation, 1-3 times higher Faraday efficiency and 1.4 times greater denitrification. Ying et al. [166], fabricated an aerogel-based anode modified by polypyrrole using paper pulp as raw materials through series processes of freeze drying and carbonization (Fig. 10c) in dual chamber MEC for degrading toluene in synthetic wastewater using microorganisms. To elucidate the role of polypyrrole coating on anode, the results were compared to graphite electrode and pure carbon aerogel. The microbial analysis indicated the abundance of microbial community abundance of *Comamonas* in pure aerogel electrode and polypyrrole/aerogel electrodes by about 17.89 % and 26.06 %, correspondingly which is well-known for its contribution in degrading toluene. Moreover, the microbial viability and quantity with respect to the biofilm thickness for the three-electrode indicated that the modified PPy/CA thickness in terms of viability and quantity significantly increased (Fig. 10d), leading to outperformance of PPys/CA over two anodes. Similarly, Feng and co-workers [173], prepared a polyaniline/CNT anode modifier on the surface of carbon cloth as anode electrode in double chamber MEC for toluene removal. The microbial analysis exhibited substantial improvement in viable biofilm and their density for the modified electrode compare the bare CC while the surface engineering of anode also boosted the two species of electroactive microorganisms: *Acinetobacter* and *Comamonas* which are well-known for degrading toxic pollutants like toluene.

Kumar and co-workers [174] proposed to improve the graphite-based anode of the MEC by coating the electrode with polyaniline to increase the rate of biohydrogen production. Interestingly, the coating process was applied in way that graphite anode immersed in as-prepared solution and stirred for 7 h to be completely covered by the polymeric modifier and they reported 30 % enhancement in rate of hydrogen production compared to the unmodified electrode.

4.9. Utilizing biocarbon composites

Li et al. [175] activated biochar by $Fe_2(SO_4)_3$ and decorated on the surface of the graphite felt anode of an MEC to improve the performance of an integrated MEC-AD wastewater treatment in comparative analysis with single AD and MEC-AD without the modified anode. The findings showed that due to the introduction of Fe-O-C functional group the rate of EET significantly increased with COD removal around 87 % which was 36 % and 20 % higher than both scenarios. The DFT analysis examined the electronic structures of phenol, quinoline, and indole explain their different degradation behaviors on the modified anode. As phenol's O—H bond is highly positive it is the easiest site for electron attack (Fig. 12a-top) while quinoline stabilizes transferred electrons at nitrogen and lower its LUMO and favoring C—H bond reduction (Fig. 12a-centered), while on the other hand indole's clustered hydrogens raise its HOMO and make the N—H bond susceptible(Fig. 12a-bottom). Hence, with $Fe_2(SO_4)_3$-modified biochar, enhanced conductivity and Fe–O–C sites promote efficient electron transfer to these vulnerable sites leading to higher pollutant degradation. Importantly, in iron-derived heteroatom doped carbon frameworks, structural motifs

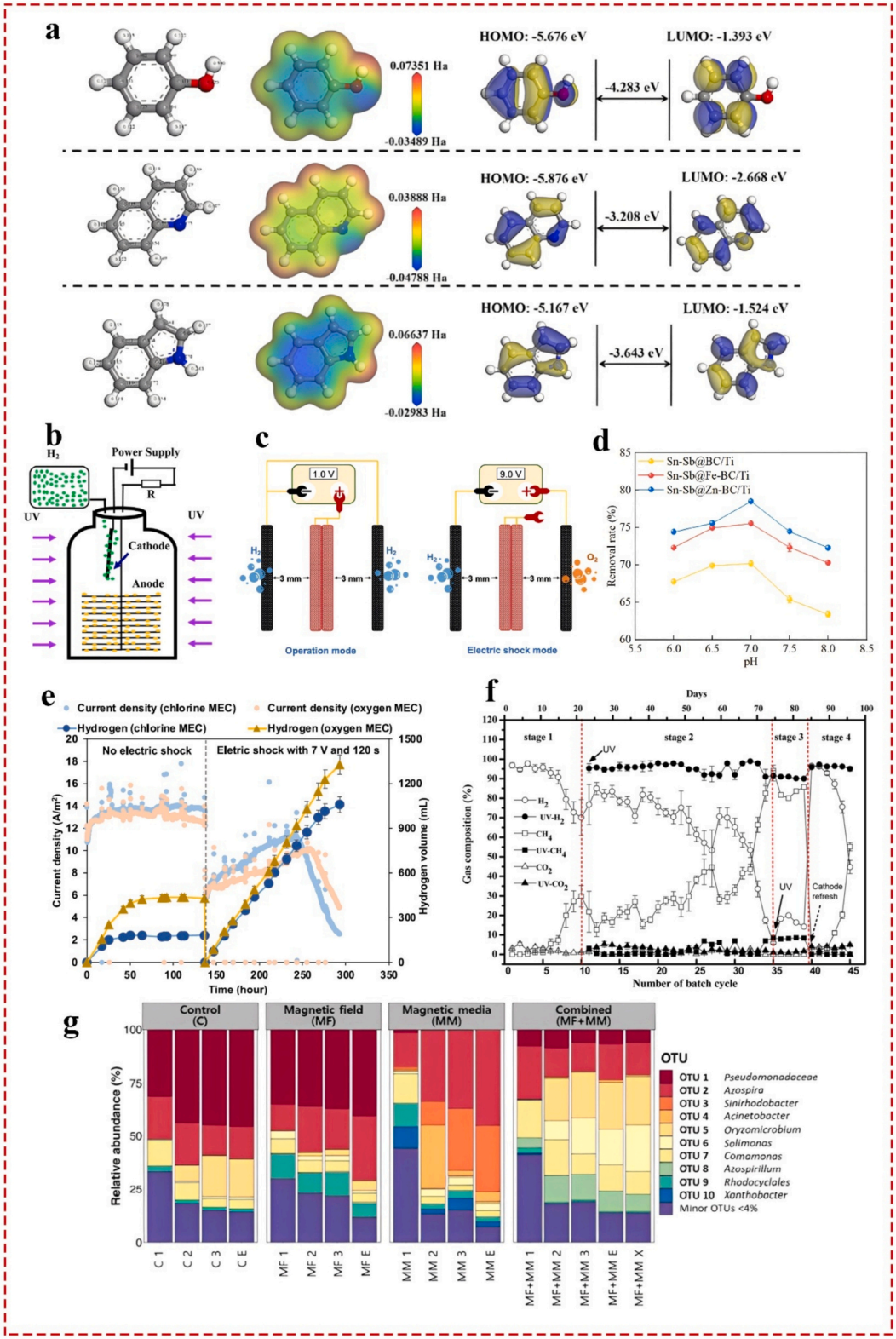

Fig. 12. a) The chemistry properties of different structure of phenol (top), quinoline (center) and indole (bottom) [175] reprinted with permission from Elsevier. b) Schematic diagram of an MEC with UV irradiation. [186] reprinted with permission from American Chemical Society. c) Schematic of the electrical connections during MEC operation mode (left), and electric shock mode (right) [189]. d) Removal rates in MEC systems at different pHs, for various compositions. [178] reprinted with permission from Elsevier. e) Effect of electric shock for oxygen or chlorine generation on H2 production and current density [189] reprinted with permission from Elsevier. f) Biogas (H2, CO2 and CH4) concentrations of MECs in the four stages. Stage 1: from cycles 1 to 10, stage 2: from cycles 11 to 35, stage 3: from cycles 36 to 39, and stage 4: from cycles 40 to 45. [186] reprinted with permission from American Chemical Society. g) Relative abundance of bacterial community operational taxonomic units (OTUs) > 4 % in at least one of the samples [190] reprinted with permission from Elsevier.

such as Fe-O-C play a crucial role in pollutant degradation via modifying the regulating the microenvironment of local electronic of Fe centres and mediate charge transfer to oxidants/contaminants through two pathways which was highlighted in previous studies [176,177]. The Fe–O–C bond creates an electronic bridge between iron active centres and the carbonaceous support facilitates rapid Fe^{3+}/Fe^{2+} redox cycling under oxidative conditions. The oxygen-linked carbon fragments adjacent to Fe serve as electron reservoirs and conductive pathways to support efficient transfer of electrons from the iron centre to the adsorbed pollutant or oxidant.

Qin et al. [178] fabricated two biochar-based anodes modified by Fe and Zn through pyrolysis, doped by Sn/SB for removal of perfluorooctanoic acid in double chamber MEC. The performance of modified anodes evaluated under different operational conditions including the variable voltage and pH and perfluorooctanoic dosages and optimal operational conditions were found. Their findings demonstrated that the removal efficiency of Zn-based electrode outperformed significantly and marginally outperformed than unmodified and Fe-based anodes respectively (Fig. 12d). Indeed, introducing the metallic nanoparticles alongside with multi-heteroatom doping of resulted in superior surface roughness/area and proliferation of microbial community and better adhesion and formation of biofilm, all together results in higher EET. However, it should be reminded that the authors did not elucidate the contribution of each metal compound in the removal efficiency as well as EET.

It is important to mention that, multiple heteroatoms doping through synergistic impact improve electrode performance in different aspects. Briefly, doping Fe creates redox-active centers that improve catalytic electron mediation and increase the density of states near the Fermi level that lead to faster electron transfer while doping Zn introduce oxygen vacancies and modulates the graphitic structure that decreasing charge-transfer resistance whereas incorporating Sn enhances hydrophilicity through surface Sn—O sites and facilitates bacterial adhesion and nutrient diffusion. Collectively, the synergies through multi-heteroatoms doping making this strategy as one of the most effective approaches toward fabricating high-performance anode and cathode electrodes.

4.10. Chemical treatment

Applying chemical treatment is an effective strategy which can indirectly improve the performance of anode electrode and EET for suppressing methanogenesis and promote hydrogen production. Among them, 2-bromoethanesulfonate (BES) has extensively used in various architectures of microbial electrochemical technologies [179–181]. For instance, Chae et al. [182] in a comparative analysis studied the effect of various methanogens inhibitions including instant changing in operational conditions including pH, temperature and exposing air as well as using BES and reported none of the physical methods significantly impacted the methanogens except BES which lead to enhancement of generated hydrogen from 56.1 ± 5.7 to 80.1 ± 6.5 % (3.2 mol-H2/mol-acetate) even after 10 batch cycles. In another study, Catal and co-workers [183] showed that adding various antibiotics in MEC including 2-chloroethane sulfonate, 2-bromoethane sulfonate, and 8-aza-hypoxanthine at optimum concentration results in simultaneous methanogens inhibition and hydrogen producers' promotion. Interestingly, the mechanistic insight behind the effectiveness of BES is that, BES is a structural analogue of coenzyme M (2-mercaptoethanesulfonate) which is the methyl carrier in the terminal step of methanogenesis. By binding to methyl-coenzyme M reductase (MCR), BES blocks the conversion of methyl-coenzyme M to methane. In this regard, BES become a competitor to all known methanogenic and suppress them without affecting non-methanogenic anaerobes. This specific inhibiting enzymatic feature distinguishes BES from other inhibitors, which they can inhibit not only methanogenic bacterial but electroactive bacteria too. Previous studies also highlighted that using chloroform at the fraction 0.02 % wt in single chamber MEC resulted in 18 % improvement in rate of biohydrogen production [149].

4.11. Irradiation treatment

Plasma treating anode electrodes enhance biofilm adhesion by modifying surface chemistry and morphology without changing bulk conductivity. The plasma treatment introduces abundant oxygen/nitrogen-containing functional groups such as –OH, –COOH, –C=O, –Nox etc. just to name a few and increases surface energy while it also boost surface roughness and porosity that also enhance effective surface area, altogether make the anode more hydrophilic and electrostatically favorable for microbial attachment. It is worth noting that, the polar groups also improve protein and EPS adsorption which has positive impact on biofilm formation.

Rozenfeld et al. [185] explored the impact of plasma-treated anodes on MEC performance by focusing on carbon cloth and stainless-steel combinations to improve biofilm formation and electron transfer efficiency. The combined plasma-treated carbon cloth and stainless steel anode demonstrated a current density of 16.36 A/m^2 at 0.6 V—three times higher than untreated setups—alongside enhanced biofilm viability (0.92 OD540). The maximum hydrogen production rate observed was around 0.0736 m^3 H_2/m^2/day which was significantly higher than untreated anode designs. It was concluded that the plasma-treated anodes foster stronger microbial attachment and bioactivity which suggested that surface modifications can considerably enhance MEC hydrogen production capabilities by improving biofilm stability and electron transfer efficiency.

Zhang and co-workers [186] suggested employing the ultraviolet irradiation for improving the performance of hydrogen production through inhibition of methanogenesis (Fig. 12b). To elucidate the role of UV on hydrogen production and preventing methene production they experiments designed in four stages which were stage 1: no UV, stage 2: the whole experiments with UV, stage 3: UV irradiation to reactor operated in the first stage and the last stage replacing the cathode with a new one to understand whether the methanogenesis of electrode is the main source methane production or not. Their findings revealed that in the beginning of the stage 1 the H2 concentration is high but after cycle 6 the CH4 increased, while throughout the stage 2 high purity H2 (>95 %) almost for 50 days was obtained with little reduction at the end of the cycle around 91 % (Fig. 12f). Interestingly, in stage 4 by refreshment of cathode and significant enhancement of H2, it was realized that methanogenesis on the surface of the electrode has the main contribution in CH4 production. One important thing that study was not highlighted is that applying UVC needs specific amount of energy which should be consider in calculation of energy recovery.

4.12. Magnetic/electric induce

Implementing magnetic field and electric pulse suggested as an effective indirect strategy to promote electroactive bacteria in the anerobic condition on electrodes in bioelechtrochemical systems. Nandy and colleagues [187] highlighted the positive role of applying electrical pulse on *E. coli* species in improving power generation of MFCs as the result of triggering electroactive features of microbial culture. Moreover, Riham et al. [188] comprehensively reviewed the role of applying magnetic field on microbial and electrogenic activity of microbial-driven electrochemical technologies. In this regard, limited studies examined these strategies on microbial electrode activities and performance of MEC. Harrison et al. [189] studied the impact of applying electrical shock imposing on electrodes to inhibit the formation of H2 scavengers(Fig. 12c). The experiments were conducted in a wide range of parameters including applied shock from 1 to 11 V for three durations of 60 s, 90 s, and 120 s in 12 h and 24 h intervals. It was realized that increasing the electrical shock with longer during at 120 s resulted in higher cathodic hydrogen recovery and minimizing the methane

hydrogen recovery accordingly. Moreover, during the electrical shock electrodes act as water splitting leading to generate oxygen and hydrogen where the experiments conducted for two sets chlorine and oxygen denoted MEC. The findings showed following electrical shock, the rate of H2 increased substantially for both the chlorine and oxygen cells, with overall production of 1059.1 ± 53.0 mL and 1328.2 ± 66.4 mL, correspondingly (Fig. 12e), which effectively eliminated methanogenesis with a limited effect on the anaerobes due to in-situ generation of chlorine and oxygen.

Park et al. [190] evaluated the effect of applying magnetic field on microbial community of anode in double chamber MEC in various scenarios which were applying magnetic field as single factor (MF), utilizing biochar modified by magnetic media (MM), and concurrent applying magnetic field and magnetic media (MFMM) and a carbon felt (CF) electrode as control. The microbial analysis based on operational taxonomic units (OUT) showed abundance of *Pseudomonadaceae* species in the scenarios of CF and MF – a well-known electroactive bacterium-higher than MM and MFMM, however, the rate of hydrogen production was 1.8-fold higher than the CF scenario. Interestingly, the relative abundance of bacterial on OUT demonstrated that the *Azospirillum* family in MFMM was remarkably higher with 12.4 %, while it was less than 1 % in the others (Fig. 12g). Based on the positive correlation between OTU6 abundance and H2 production, *Azospirillum* was responsible for the high efficiency of the MF + MM reactor. This is consistent with previous findings that *Azospirillum* is a frequently detected EAB in MEC and MFC systems.

In Table 1, it is important to point out that the produced hydrogen is reported with different dimensions which is attributed to the target of study. As it can be seen, in numerous studies the hydrogen production reported based on the volume of the reactor, however, in a few studies it reported based on the rate of substrates consumption, COD removal and electrodes surface area. Last but not least, in number of studies, authors did not report the produced hydrogen because the target of studies were pollutant removal.

5. Summaries, challenges and future directions

Based on the discussion in this critical review, the following could be summarized as the current status, challenges and future directions:

- To understand the impact various adopted strategies on anode electrodes, applying electrochemical tests such as CV, EIS, DPV, LSV is pivotal, particularly for comparative study using physical strategies (3D network, Irradiation etc.) or chemical treatment and utilizing functional materials where it is important to find the optimum values and fractions of different elements. As can be seen (Table 1) these analyses in numerous research, were not applied which highly recommended for future studies at least one or a number of them accordingly.
- As engineering EET is directly related to the biofilm, conducting advanced characterization methods like CLSM is of great importance to highlight the formation of biofilm as well as living dead cells to demonstrate the effectiveness of adopted strategies on biofilm promotion.
- Employing recently developed approaches such as Electrode Potential Slope (EPS) method which can calculate the internal resistance of MEC like electrodes, electrolyte membranes [134] is highly recommended to understand the contribution of each component in total resistance. This is particularly important as the highest portion of internal resistance in MEC is associated by the anode electrode which can be used as powerful tool to regulate anode resistance.
- To reduce the anode resistance several easy-to-apply methods such as regulating the anode-to-cathode ratio, introducing fluid motion in the chamber (particularly in single chamber), finding the optimum distance between electrodes could be adopted. Moreover, to reduce anode resistance several easy-to-apply methods such as the regulating anode-to-cathode ratio, introducing fluid motion in the chamber (particularly in single chamber), finding the optimum distance between electrodes could be adopted.
- The anode thickness is a crucial factor in system performance. Although the thickness of anode based on the experiments in the literature exhibited in a limited number of studies, any thickness between 2 and 5 mm would be appropriate for carbon-based anodes, which also validated by theoretical simulations [137]. However, it is highly desirable to conduct simulation studies to understand the optimum thickness of anode not only for the lab-scale experiments, but in the large-scale systems for carbon or metal anodes.
- The ratio of anode to cathode found as an important factor for superior EET. Generally, the ratio of anode at least should be equal to cathode electrode for effective EET while in some studies the larger anode-to-cathode ratio exhibited higher current densities.
- During the acclimation of anode, it is crucial to promote and growth the microbial communities with the dose that the biofilm is going to work in the MEC because high amount of substrate could result to formation of different microbial species (Such as high abundance of methanogens) which is not desirable for the main purpose of MEC.
- Anodes arrangement in the MEC should be carefully designed, particularly for those configurations which use multi-anode in sequence because the higher densities were produced by the anode closest to the cathode [137].
- For scenarios which a 3D anode fabricated (through methods like 3D printing), the design, shape and geometry should be in a way that the electrode-electrolyte interaction reach to the highest value since improper design may result in higher resistance leading to the lower charge transfer and diffusion. Thus, when applying this strategy, it is highly recommended to experiment different approaches to find the optimum geometry/shape of anode electrode.
- Among various nanoparticles, Fe due to its crucial role in microbial metabolism is the most utilized element while other nanomaterials are overlooked. Nanostructures materials such as modified anodes by graphene in MEC demonstrated to enrich the biofilm with superior EET. Considering the high potential of biocompatible nanomaterials such as Fe and graphene the number of studies in this context is very limited. On the other side of the coin, to elucidate the practicality of these materials it is high recommended to conduct experiment with complex wastewater rather than synthetic mediums.
- Although applying nanomaterials exhibited significant improvement in anode performance, it should be reminded that, nanomaterials beyond their optimum dosage might have adverse effects on biofilm (generally it could be highly toxic biological systems [191]) and decrease the rate of hydrogen production accordingly. Thus, for applying a strategy like using metallic nanomaterials it is pivotal to find the optimum concentration for boosting synergies and managing trade-offs.
- Although some strategies such as encapsulation exhibited to boost electroactive biofilm species and improve the overall performance of anode, they are generally applicable for primary and lab-scale studies rather than large-scale scenarios, because of technological and economic barriers. The same is true for research that use pure culture (such as *Geobacter sulfurreducens*) for biofilm growth as this condition could not happen in real-world.
- The interaction between toxic nanomaterials and biofilm in MECs was limitedly studied with only one research highlight the role of Ag nanoparticle on biofilm. Hence, it is high recommended to study the role of other abundantly spread toxic nanomaterials such as copper, chromium, cadmium etc. with biofilm, as these toxic materials are widely spread in the environment. Finally, it could be an interesting research direction to study the effect of various morphologies and different size of toxic nanomaterials with biofilm as changing these parameters are highly influential on biological systems.
- The number of theoretical studies on the interaction of the biofilm and anode electrode in MECs are limited which make it necessary to

Table 1
Summary of applied anode features where physical modifications applied.

Method of modification	Systems configuration	Reactor volume	Type of anode	Type of wastewater	Anode thickness	H2 production	Electrochemical analysis applied	Ref
Regulating resistance	Single chamber	320	Carbon cloth	Synthetic wastewater	–	3.7 L-H_2/L liquid/day	EIS	[133]
Regulating resistance	Double chamber	14	Carbon felt	Synthetic wastewater	6.35 mm	NA	–	[134]
Regulating resistance	Single chamber	28	Graphite brush	Synthetic wastewater	–	NA	–	[135]
Promoting 3D network	Double chamber	80	Not explicitly mentioned	Various cheeses wastewater	NA	5 mL/70 min 5 mL/85 min 5 mL/120 min (for different wastewater)	CV, EIS and LSV	[136]
Promoting 3D network	Double chamber	N/A	Graphite	Theoretical study	0–40 mm	NA	Theoretical study	[137]
Promoting 3D network	Double chamber	1560	3D-weaved carbon mesh	Synthetic wastewater	N/A	0.123 m^3 H_2/m^3 wastewater/day	CV, EIS and LSV	[138]
Promoting 3D network	Double chamber	1560	3D-weaved carbon mesh	Synthetic wastewater	N/A	2.89 ± 0.18 m^3 H_2/m^3 wastewater·day	CV, EIS and LSV	[139]
Anode arrangement	Single chamber	200	Graphite fiber + iron	Synthetic wastewater	N/A	183.83 mL·H_2/day	CV, EIS	[141]
Acclimation procedure	Single chamber	64	Graphite felt	Corn stalk fermentation effluent	N/A	4.52 ± 0.13 m^3 H_2/m^3 wastewater/day	CV	[142]
Acclimation procedure	Single chamber	5	Carbon fiber brush	Synthetic wastewater	3.2	352 mL H_2/g COD	None	[143]
Anode arrangement	Single chamber	50-100	Carbon felt	Synthetic wastewater	5 mm	83–272 mL H_2/day	–	[144]
Anode arrangement	Single chamber	64	Graphite felt	Synthetic wastewater	5 mm	5.56 m^3 H_2/m^3·reactor·day	EIS and CV	[145]
Anode arrangement	Single chamber	64	Graphite felt	Synthetic wastewater	5 mm	2.39 m^3 H_2/m^3·reactor/day	None	[146]
Anode arrangement	Single chamber	64	Graphite felt	Corn dark fermented effluent	5 mm	3.43 m^3 H_2/m^3·reactor/day	CV	[147]
Electrode ratio	Single chamber	8	Graphite plate	Synthetic wastewater	3.2 mm	N/A	None	[148]
Encapsulation	Semi-Single chamber	400	Carbon cloth	Actual wastewater	N/A	0.16 ± 0.009 m^3 H_2/m^2·anode·day	LSV	[153]
Encapsulation	Single chamber	100	Carbon cloth	Wastewater, *Geobacter* medium	N/A	0.56 m^3 H_2/m^3·reactor·day	LSV	[154]
Encapsulation	Single chamber	100	Carbon cloth	Synthetic wastewater	N/A	0.017 m^3 H_2/m^3·reactor·day	LSV	[155]
Encapsulation	Single chamber	100	Graphite particle	Synthetic wastewater	–	0.076 m^3 H_2/m^3·reactor·day	CV, EIS	[156]
Encapsulation	Single chamber	100	Carbon cloth	*Geobacter* medium	–	0.82 m^3 H_2/m^3·reactor·day	CV, EIS, LSV	[157]
Encapsulation	Single chamber	100	Carbon Cloth+ alginate	Synthetic wastewater	–	0.42 m^3 H_2/m^3·reactor·day	CV, EIS, LSV	[157]
Functional materials	Single chamber	440	Graphene Paper	Synthetic wastewater	N/A	224 mL H_2/g·biomass	CV and EIS	[158]
Functional materials	Single chamber	250	Carbon brush	River mud	N/A	NA	CV	[160]
Functional materials	–	–	Graphite disk		N/A	NA	None	[161]
Functional nanomaterials	Single chamber	300	Stainless steel	Synthetic wastewater	N/A	637 mL H_2/batch 827 mL H_2/batch (Al_2O_3)	–	[165]
Functional materials	Single chamber	300	Stainless steel	Synthetic wastewater	N/A	700–800 mL H_2/batch (MgO)	–	[165]
Functional nanomaterials	Single chamber	300	Stainless steel	Synthetic wastewater	N/A	827 mL H_2/batch (Fe_2O_3)	–	[165]
Functional nanomaterials	Single chamber	500	N-doped CNT	Brewery wastewater		21 L-H_2/L-reactor/day	–	[167]
Polymer modification	Single chamber	100	Graphite plate	Fertilizer liquid waste	0.32 cm	NA	–	[171]
Polymer modification	Double chamber	570	Carbon rod	Synthetic wastewater	–	NA	CV	[172]
Polymer modification	Double chamber	100	Carbon aerogel	Synthetic wastewater	–	NA	–	[166]
Polymer modification	Single chamber	–	Graphite felt	Synthetic wastewater	–	NA	–	[174]
Utilizing biochar	Single chamber	4000	Graphite felt	Coal wastewater	–	NA	–	[175]
Utilizing biochar	Double chamber		Modified biocarbon	Wastewater with PFOA	0.5 mm	NA	CV, CAP	[178]
Chemical treatment	Double chamber	200	Carbon felt	Synthetic wastewater	–	30.1 mL H_2/batch	–	[181]
Chemical treatment	Double chamber	200	Carbon felt	Synthetic wastewater	–	3.2 mol H2/mol-acetate	–	[182]

(*continued on next page*)

Table 1 (*continued*)

Method of modification	Systems configuration	Reactor volume	Type of anode	Type of wastewater	Anode thickness	H2 production	Electrochemical analysis applied	Ref
Chemical treatment	Single chamber	500	Carbon felt	Synthetic wastewater	–	18 mL H_2/batch	–	[183]
Irradiation	Single chamber	320	Carbon cloth	Synthetic wastewater	N/A	0.0736 m^3 H_2/m^2-electrode/day	DPV, LSV	[185]
Irradiation	Single chamber	130	Graphite brush	Synthetic wastewater	4 cm	3.70 ± 0.11 mol H_2/mol acetate	–	[186]
Magnetic/electric induce	Single chamber	300	Carbon cloth	Synthetic wastewater	2.5–5.1 mm	1.62 ± 0.16 L-H_2/L-reactor/day	–	[189]
Magnetic/electric induce	Double chamber	160	Biocarbon	Synthetic wastewater	–	14.59–26.5 mL H_2/Volume-reactor	–	[190]
Magnetic/electric induce	Double chamber	160	Biocarbon	Synthetic wastewater	–	23.02–32.73 mL H_2/Volume-reactor	–	[190]

conduct more theoretical analysis. However, one important factor is to implement the right mechanism of EET in biofilm which determined that occur via the third EET mechanisms through nanowires [78,79,89].

- It is crucially important to note that, these strategies are not mutually exclusive, rather, by combining them it is possible to reach superior EET in anodes [139,157,190] than adopting single strategy. Thus, it is highly recommended to integrate the above-mentioned strategies through rational design to improve the performance of anodes rate of hydrogen production.
- By employing some types of conductive polymers like polypyrrole and polyaniline etc., [166,171,172] it is possible to promote specific types of microorganism not for hydrogen production but for degrading specific pollutants. Regarding the high potential of polymers as dual-functional strategy for hydrogen production and pollutant removal there are a lot of room for utilizing other conductive polymers such as Poly(3,4-ethylenedioxythiophene)-PEDOT- not only as anode modifier but to compare their effectiveness from different aspects whether the rate of H_2 production or pollutant removal.
- As irradiating MEC's bioreactor by UVC wavelengths (100-280 nm) demonstrated exceptional results in inhibiting methanogens and improved hydrogen production, it is highly recommended to examine the effect of UVB wavelengths (280-315 nm) as the methanogens inhibitor because of the lower energy required for UVB. More interestingly, such experiment could be conduct in comparative analysis with UVC to highlight the strength of each method accordingly.
- It should be reminded that when adopting strategies that require consuming electrical energy such as UV irradiation or magnetic field [189,190], the amount of utilized electrical energy should be consider in calculation of MEC metrics such as of energy recovery.
- Sometimes employing a strategy result in suppressing well-known electroactive bacteria like *Pseudomonadaceae* on anode but the system still generates higher hydrogen due to promoting another specific electroactive bacterium like *Azospirillum* [190]. This is highlighted the significance of engineering microbial communities in EET through applying specific strategies for targeting to colonize specific high-efficient microorganism to boost hydrogen production.

CRediT authorship contribution statement

Seyed Masoud Parsa: Writing – original draft, Validation, Resources, Methodology, Formal analysis, Data curation. **Huu Hao Ngo:** Writing – review & editing, Supervision, Project administration, Data curation, Conceptualization. **Bing-Jie Ni:** Writing – review & editing, Supervision, Resources, Methodology. **Xinbo Zhang:** Writing – review & editing, Visualization, Validation. **Ying Liu:** Writing – review & editing, Visualization, Data curation. **Li Luo:** Writing – review & editing, Validation, Formal analysis. **Hui Cheng:** Visualization, Validation, Resources. **Wenshan Guo:** Writing – review & editing, Supervision, Resources, Project administration, Data curation, Conceptualization.

Declaration of Generative AI and AI-assisted technologies in the writing process

During the preparing the first revision of this work, the authors used Chat-GPT Version5 to polish the language of manuscript and improving readability. All grammatical changes by AI were reviewed and edited by the authors accordingly.

Declaration of competing interest

The authors declare that they have no known competing financial interests or personal relationships that could have appeared to influence the work reported in this paper.

One of the co-authors in this review paper, Prof. Wenshan Guo, is the CEJ's editor.

Acknowledgements

This research was supported by University of Technology Sydney, Australia (UTS, RIA NGO and UTS NM GUO).

Data availability

Data will be made available on request.

References

[1] UN General Assembly, Resolution Adopted by the General Assembly on 25 September 2015, Transforming Our World: The 2030 Agenda for Sustainable Development, 16301, 2015, pp. 1–35, https://doi.org/10.1007/s13398-014-0173-7.2.

[2] S.M. Parsa, F. Norozpour, A. Hedayatizadeh, D. Javadi, S. Shoeibi, H. Kargarsharifabad, S. Feng, W. Guo, H.H. Ngo, B.J. Ni, Understanding the role of small-scale solar desalination (solar still, humidification-dehumidification) to achieving sustainable development goals (SDGs) in developing nations: a review, Sustain. Energy Technol. Assess. 81 (2025), https://doi.org/10.1016/j.seta.2025.104423.

[3] S.M. Parsa, A. Rahbar, M.H. Koleini, Y. Davoud Javadi, M. Afrand, S. Rostami, M. Amidpour, First approach on nanofluid-based solar still in high altitude for water desalination and solar water disinfection (SODIS), Desalination 491 (2020) 114592, https://doi.org/10.1016/j.desal.2020.114592.

[4] F. Fuso Nerini, J. Tomei, L.S. To, I. Bisaga, P. Parikh, M. Black, A. Borrion, C. Spataru, V. Castán Broto, G. Anandarajah, B. Milligan, Y. Mulugetta, Mapping synergies and trade-offs between energy and the Sustainable Development Goals, Nat. Energy 3 (2018) 10–15, https://doi.org/10.1038/s41560-017-0036-5.

[5] S.M. Parsa, A. Rahbar, M.H. Koleini, S. Aberoumand, M. Afrand, M. Amidpour, A renewable energy-driven thermoelectric-utilized solar still with external condenser loaded by silver/nanofluid for simultaneously water disinfection and desalination, Desalination (2020) 114354, https://doi.org/10.1016/j.desal.2020.114354.

[6] S.M. Parsa, F. Norozpour, A.H. Elsheikh, A.E. Kabeel, Solar desalination/purification (solar stills, humidification-dehumidification, solar disinfection) in high altitude during COVID19: insights of gastrointestinal manifestations and systems' mechanism, J. Hazard. Mater. Adv. 10 (2023) 100259, https://doi.org/10.1016/j.hazadv.2023.100259.

[7] S.M. Parsa, Mega-scale desalination efficacy (Reverse Osmosis, Electrodialysis, Membrane Distillation, MED, MSF) during COVID-19: evidence from salinity, pretreatment methods, temperature of operation, J. Hazard. Mater. Adv. 9 (2023) 100217, https://doi.org/10.1016/j.hazadv.2022.100217.

[8] H. Liu, S. Grot, B.E. Logan, Electrochemically assisted microbial production of hydrogen from acetate, Environ. Sci. Technol. 39 (2005) 4317–4320, https://doi.org/10.1021/es050244p.

[9] R.A. Rozendal, H.V.M. Hamelers, G.J.W. Euverink, S.J. Metz, C.J.N. Buisman, Principle and perspectives of hydrogen production through biocatalyzed electrolysis, Int. J. Hydrog. Energy 31 (2006) 1632–1640, https://doi.org/10.1016/j.ijhydene.2005.12.006.

[10] A. Kadier, M. Sahaid, P. Abdeshahian, K. Chandrasekhar, A. Mohamed, N. Farhana, W. Logroño, Y. Simayi, A. Abdul, Recent advances and emerging challenges in microbial electrolysis cells (MECs) for microbial production of hydrogen and value-added chemicals, Renew. Sust. Energ. Rev. 61 (2016) 501–525, https://doi.org/10.1016/j.rser.2016.04.017.

[11] M. Kitching, R. Butler, E. Marsili, Enzyme and microbial technology microbial bioelectrosynthesis of hydrogen: current challenges and scale-up, Enzym. Microb. Technol. 96 (2017) 1–13, https://doi.org/10.1016/j.enzmictec.2016.09.002.

[12] M.Z. Khan, A.S. Nizami, M. Rehan, O.K.M. Ouda, S. Sultana, I.M. Ismail, K. Shahzad, Microbial electrolysis cells for hydrogen production and urban wastewater treatment: a case study of Saudi Arabia, Appl. Energy 185 (2017) 410–420, https://doi.org/10.1016/j.apenergy.2016.11.005.

[13] R. Rousseau, L. Etcheverry, E. Roubaud, R. Basséguy, M. Délia, A. Bergel, Microbial electrolysis cell (MEC): strengths, weaknesses and research needs from electrochemical engineering standpoint, Appl. Energy 257 (2020) 113938, https://doi.org/10.1016/j.apenergy.2019.113938.

[14] N. Zhao, D. Liang, S. Meng, X. Li, Bibliometric and content analysis on emerging technologies of hydrogen production using microbial electrolysis cells, Int. J. Hydrog. Energy 45 (2020) 33310–33324, https://doi.org/10.1016/j.ijhydene.2020.09.104.

[15] N. Wrana, R. Sparling, N. Cicek, D.B. Levin, Hydrogen gas production in a microbial electrolysis cell by electrohydrogenesis, J. Clean. Prod. 18 (2010) S105–S111, https://doi.org/10.1016/j.jclepro.2010.06.018.

[16] L. Lu, Z.J. Ren, Microbial electrolysis cells for waste biorefinery: a state of the art review, Bioresour. Technol. 215 (2016) 254–264, https://doi.org/10.1016/j.biortech.2016.03.034.

[17] D. Cheng, H. Hao, W. Guo, S. Woong, D. Duc, Impact factors and novel strategies for improving biohydrogen production in microbial electrolysis cells, Bioresour. Technol. 346 (2022) 126588, https://doi.org/10.1016/j.biortech.2021.126588.

[18] R. Gautam, J.K. Nayak, N.V. Ress, R. Steinberger-wilckens, U. Kumar, Biohydrogen production through microbial electrolysis cell : structural components and influencing factors, Chem. Eng. J. 455 (2023) 140535, https://doi.org/10.1016/j.cej.2022.140535.

[19] N. Yasri, E.P.L. Roberts, S. Gunasekaran, The electrochemical perspective of bioelectrocatalytic activities in microbial electrolysis and microbial fuel cells, Energy Rep. 5 (2019) 1116–1136, https://doi.org/10.1016/j.egyr.2019.08.007.

[20] D. Radhika, A. Shivakumar, D.R. Kasai, R. Koutavarapu, S.G. Peera, Microbial electrolysis cell as a diverse technology: overview of prospective applications, advancements, and challenges, Energies 15 (7) (2022) 2611.

[21] B.E. Logan, K. Rabaey, Conversion of wastes into bioelectricity and chemicals by using microbial electrochemical technologies, Science (1979) 686 (2012), https://doi.org/10.1126/science.1217412.

[22] M. Muddasar, A. Aslam, K. Latif, Performance efficiency comparison of microbial electrolysis cells for sustainable production of biohydrogen — a comprehensive review, Int. J. Energy Res. (2022) 5625–5645, https://doi.org/10.1002/er.7606.

[23] T. Hua, S. Li, F. Li, Q. Zhou, B.S. Ondon, Microbial electrolysis cell as an emerging versatile technology: a review on its potential application, advance and challenge, J. Chem. Technol. Biotechnol. (2019) 1697–1711, https://doi.org/10.1002/jctb.5898.

[24] A. Bashaa, A. Khalila, R. Mohammed, Wastewater treatment and hydrogen production via microbial electrolysis cells (MECS) and fermentation methods: a comparative review, J. Contemp. Technol. Appl. Eng. 2 (2023) 29–41, https://doi.org/10.21608/JCTAE.2023.218803.1014.

[25] T. Fudge, I. Bulmer, K. Bowman, S. Pathmakanthan, W. Gambier, Z. Dehouche, S. M. Al-salem, A. Constantinou, Microbial electrolysis cells for decentralised wastewater treatment: the next steps, Water 13 (4) (2021) 445.

[26] N. Savla, M. Guin, S. Pandit, H. Malik, Recent advancements in the cathodic catalyst for the hydrogen evolution reaction in microbial electrolytic cells, Int. J. Hydrog. Energy 47 (2022) 15333–15356, https://doi.org/10.1016/j.ijhydene.2022.03.058.

[27] C. Rao, Z. Zhao, Z. Wen, Q. Xu, K. Chen, H. Chen, S. Ci, N-doped Mo 2 C particles as a cathode catalyst of asymmetric neutral-alkaline microbial electrolysis cells for hydrogen production, Sustain. Energy Fuels (2023) 3375–3383, https://doi.org/10.1039/d3se00597f.

[28] Z. Liu, L. Zhou, Q. Chen, W. Zhou, Y. Liu, Advances in graphene/graphene composite based microbial fuel/electrolysis cells, Electroanalysis (2017) 652–661, https://doi.org/10.1002/elan.201600502.

[29] T.E. Suharto, I. Satar, W.R.W. Daud, M.R. Somalu, K. Byung, Hong, recent advancement of nickel based-cathode for the microbial electrolysis cell (MEC) and its future prospect, J. Eng. Sci. Technol. Rev. 15 (2022) 191–198, https://doi.org/10.25103/jestr.151.24.

[30] D. Frattini, G. Karunakaran, E.B. Cho, Y. Kwon, Sustainable syntheses and sources of nanomaterials for microbial fuel/electrolysis cell applications: an overview of recent progress, Processes 9 (2021), https://doi.org/10.3390/pr9071221.

[31] B. Kim, E. Yang, B. Kim, M. Obaid, J.K. Jang, K.J. Chae, Recent application of nanomaterials to overcome technological challenges of microbial electrolysis cells, Nanomaterials 12 (2022) 1–23, https://doi.org/10.3390/nano12081316.

[32] N.K. Abd-Elrahman, N. Al-Harbi, Y. Al-Hadeethi, A.B. Alruqi, H. Mohammed, A. Umar, S. Akbar, Influence of nanomaterials and other factors on biohydrogen production rates in microbial electrolysis cells—a review, Molecules 27 (2022) 1–24, https://doi.org/10.3390/molecules27238594.

[33] A. Kundu, J.N. Sahu, G. Redzwan, M.A. Hashim, An overview of cathode material and catalysts suitable for generating hydrogen in microbial electrolysis cell, Int. J. Hydrog. Energy 38 (2013) 1745–1757, https://doi.org/10.1016/j.ijhydene.2012.11.031.

[34] J. Tang, Y. Bian, S. Jin, D. Sun, Z.J. Ren, Cathode material development in the past decade for H2 production from microbial electrolysis cells, ACS Environ. Au 2 (2022) 20–29, https://doi.org/10.1021/acsenvironau.1c00021.

[35] M. Aysla Costa De Oliveira, A. D'Epifanio, H. Ohnuki, B. Mecheri, Platinum group metal-free catalysts for oxygen reduction reaction: applications in microbial fuel cells, Catalysts 10 (2020) 1–22, https://doi.org/10.3390/catal10050475.

[36] M. Hasany, M.M. Mardanpour, S. Yaghmaei, Biocatalysts in microbial electrolysis cells: a review, Int. J. Hydrog. Energy 41 (2016) 1477–1493, https://doi.org/10.1016/j.ijhydene.2015.10.097.

[37] R. Lin, L. Xie, X. Zheng, D. on D. Patience, X. Duan, Advances and challenges in biocathode microbial electrolysis cells for chlorinated organic compounds degradation from electroactive perspectives, Sci. Total Environ. 905 (2023) 167141, https://doi.org/10.1016/j.scitotenv.2023.167141.

[38] T. Jafary, W.R.W. Daud, M. Ghasemi, B.H. Kim, J. Md Jahim, M. Ismail, S.S. Lim, Biocathode in microbial electrolysis cell; present status and future prospects, Renew. Sust. Energ. Rev. 47 (2015) 23–33, https://doi.org/10.1016/j.rser.2015.03.003.

[39] B.H. Kim, S.S. Lim, W.R.W. Daud, G.M. Gadd, I.S. Chang, The biocathode of microbial electrochemical systems and microbially-influenced corrosion, Bioresour. Technol. 190 (2015) 395–401, https://doi.org/10.1016/j.biortech.2015.04.084.

[40] A. Thanarasu, K. Periyasamy, S. Subramanian, An integrated anaerobic digestion and microbial electrolysis system for the enhancement of methane production from organic waste: fundamentals, innovative design and scale-up deliberation, Chemosphere 287 (2022) 131886, https://doi.org/10.1016/j.chemosphere.2021.131886.

[41] F. Ndayisenga, Z. Yu, J. Zheng, B. Wang, H. Liang, I. Ali, T. Habiyakare, D. Zhou, Microbial electrohydrogenesis cell and dark fermentation integrated system enhances biohydrogen production from lignocellulosic agricultural wastes: substrate pretreatment towards optimization, Renew. Sust. Energ. Rev. 145 (2021) 111078, https://doi.org/10.1016/j.rser.2021.111078.

[42] P. Srivastava, E. Garcı, Quismondo Jesu's Palma, C. Gonzalez-Fernandez, Coupling Dark Fermentation and Microbial Electrolysis Cells for Higher Hydrogen Yield: Technological Competitiveness and Challenges, 2023, https://doi.org/10.1016/j.ijhydene.2023.04.293.

[43] W. Wang, D. Lee, Z. Lei, Integrating anaerobic digestion with microbial electrolysis cell for performance enhancement: a review, Bioresour. Technol. 344 (2022) 126321, https://doi.org/10.1016/j.biortech.2021.126321.

[44] P. Bakonyi, G. Kumar, L. Koók, G. Tóth, T. Rózsenberszki, Microbial electrohydrogenesis linked to dark fermentation as integrated application for enhanced biohydrogen production: a review on process characteristics, experiences and lessons, Bioresour. Technol. 251 (2018) 381–389, https://doi.org/10.1016/j.biortech.2017.12.064.

[45] Q. Huang, Y. Liu, B.R. Dhar, A critical review of microbial electrolysis cells coupled with anaerobic digester for enhanced biomethane recovery from high-strength feedstocks, Crit. Rev. Environ. Sci. Technol. 0 (2020) 1–40, https://doi.org/10.1080/10643389.2020.1813065.

[46] Z. Yu, X. Leng, S. Zhao, J. Ji, T. Zhou, A. Khan, A review on the applications of microbial electrolysis cells in anaerobic digestion, Bioresour. Technol. 255 (2018) 340–348, https://doi.org/10.1016/j.biortech.2018.02.003.

[47] M. Zhou, H. Wang, J. Hassett, T. Gu, Recent advances in microbial fuel cells (MFCs) and microbial electrolysis cells (MECs) for wastewater treatment, bioenergy and bioproducts, J. Chem. Technol. Biotechnol. (2013), https://doi.org/10.1002/jctb.4004.

[48] L.S. Jensen, C. Kaul, N.B. Juncker, M.H. Thomsen, T. Chaturvedi, Biohydrogen production in microbial electrolysis cells utilizing organic residue feedstock: a review line, Energies 15 (22) (2022) 8396.

[49] J.H. Tang, A review of suitable substrates for hydrogen production in microbial electrolysis cells, IOP Conf. Ser. Earth Environ. Sci. (2021), https://doi.org/10.1088/1755-1315/621/1/012145.

[50] A. Kadier, Y. Simayi, M. Sahaid, P. Abdeshahian, A. Abdul, A review of the substrates used in microbial electrolysis cells (MECs) for producing sustainable and clean hydrogen gas, Renew. Energy 71 (2014) 466–472, https://doi.org/10.1016/j.renene.2014.05.052.

[51] K. He, W. Li, L. Tang, W. Li, S. Lv, D. Xing, Suppressing methane production to boost high-purity hydrogen production in microbial electrolysis cells, Environ. Sci. Technol. (2022), https://doi.org/10.1021/acs.est.2c02371.

[52] A. Kadier, M. Sahaid, K. Chandrasekhar, G. Mohanakrishna, G. Dattatraya, R. Ganesh, G. Kumar, A. Pugazhendhi, P. Sivagurunathan, Surpassing the current limitations of high purity H2 production in microbial electrolysis cell (MECs): strategies for inhibiting growth of methanogens, Bioelectrochemistry 119 (2018) 211–219, https://doi.org/10.1016/j.bioelechem.2017.09.014.

[53] R. Karthikeyan, K. Yu, A. Selvam, A. Bose, J.W.C. Wong, Bioelectrohydrogenesis and inhibition of methanogenic activity in microbial electrolysis cells - a review,

Biotechnol. Adv. 35 (2017) 758–771, https://doi.org/10.1016/j.biotechadv.2017.07.004.
[54] B.E. Logan, Electroactive microorganisms in bioelectrochemical systems, Nat. Rev. Microbiol. 17 (2019) 307–319, https://doi.org/10.1038/s41579-019-0173-x.
[55] K. Rabaey, R.A. Rozendal, Microbial electrosynthesis — revisiting the electrical route for microbial production, Nat. Rev. Microbiol. 8 (2010) 706–716, https://doi.org/10.1038/nrmicro2422.
[56] P.D. Kiely, J.M. Regan, B.E. Logan, The electric picnic: synergistic requirements for exoelectrogenic microbial communities, Curr. Opin. Biotechnol. 22 (2011) 378–385, https://doi.org/10.1016/j.copbio.2011.03.003.
[57] A. Bora, K. Mohanrasu, T.A. Swetha, V. Ananthi, R. Sindhu, N. Thuy, L. Chi, A. Pugazhendhi, A. Arun, T. Mathimani, Microbial electrolysis cell (MEC): reactor configurations, recent advances and strategies in biohydrogen production, Fuel 328 (2022) 125269, https://doi.org/10.1016/j.fuel.2022.125269.
[58] A. Kadier, Y. Simayi, P. Abdeshahian, N. Farhana, K. Chandrasekhar, M. Sahaid, A comprehensive review of microbial electrolysis cells (MEC) reactor designs and configurations for sustainable hydrogen gas production, Alex. Eng. J. 55 (2016) 427–443, https://doi.org/10.1016/j.aej.2015.10.008.
[59] D. Leicester, J. Amezaga, E. Heidrich, Is bioelectrochemical energy production from wastewater a reality? Identifying and standardising the progress made in scaling up microbial electrolysis cells, Renew. Sust. Energ. Rev. 133 (2020) 110279, https://doi.org/10.1016/j.rser.2020.110279.
[60] S. Park, P.P. Rajesh, Y. Sim, D.A. Jadhav, Addressing scale-up challenges and enhancement in performance of hydrogen-producing microbial electrolysis cell through electrode modifications, Energy Rep. 8 (2022) 2726–2746, https://doi.org/10.1016/j.egyr.2022.01.198.
[61] E. Yang, H. Omar Mohamed, S.G. Park, M. Obaid, S.Y. Al-Qaradawi, P. Castaño, K. Chon, K.J. Chae, A review on self-sustainable microbial electrolysis cells for electro-biohydrogen production via coupling with carbon-neutral renewable energy technologies, Bioresour. Technol. 320 (2021), https://doi.org/10.1016/j.biortech.2020.124363.
[62] X. Wu, D. Ph, W. Xie, J. Ye, D. Ph, D. Sun, T. Ohnuki, D. Ph, M. Li, D. Ph, X. Zhang, D. Ph, Q. Fang, D. Ph, Q. Tang, D. Li, Progress in heavy metals-containing wastewater treatment via microbial electrolysis cell: a review, J. Water Process Eng. 55 (2023), https://doi.org/10.1016/j.jwpe.2023.104228.
[63] X. Cao, X. Huang, P. Liang, N. Boon, M. Fan, L. Zhang, X. Zhang, A completely anoxic microbial fuel cell using a photo-biocathode for cathodic carbon dioxide reduction, Energy Environ. Sci. 2 (2009) 498–501, https://doi.org/10.1039/b901069f.
[64] J. Ma, J. Zhang, Y. Zhang, Q. Guo, T. Hu, H. Xiao, W. Lu, J. Jia, Progress on anodic modification materials and future development directions in microbial fuel cells, J. Power Sources 556 (2023) 232486, https://doi.org/10.1016/j.jpowsour.2022.232486.
[65] X. Fan, Y. Zhou, X. Jin, R. Song, Z. Li, Q. Zhang, Carbon material - based anodes in the microbial fuel cells, Carbon Energy (2021) 449–472, https://doi.org/10.1002/cey2.113.
[66] C. Li, S. Cheng, Functional group surface modifications for enhancing the formation and performance of exoelectrogenic biofilms on the anode of a bioelectrochemical system, Crit. Rev. Biotechnol. 0 (2019) 1–16, https://doi.org/10.1080/07388551.2019.1662367.
[67] X. Liu, P. Qi, X. Li, P. Gao, Y. Nie, X. lei Wu, Bidirectional extracellular electron transfer modulates heterotrophic CO2 fixation in *Rhodopseudomonas palustris*, Chem. Eng. J. 516 (2025), https://doi.org/10.1016/j.cej.2025.164069.
[68] Y. Li, J. Zhang, Q. Chen, S. Tang, Y. Peng, Role of mtr pathway in extracellular electron transfer-driven malathion degradation by *Shewanella oneidensis* MR-1, Chem. Eng. J. 520 (2025), https://doi.org/10.1016/j.cej.2025.166288.
[69] H. Lv, Z. Cui, Q. Zhao, C. Zhang, B. Cui, D. Zhou, Optimal loading of α-Fe_2O_3 continually promotes microbial metabolism and extracellular electron transfer in the iron-reducing bacteria-driven microbial electro-Fenton system, Chem. Eng. J. 523 (2025) 167876, https://doi.org/10.1016/j.cej.2025.167876.
[70] dos S.A.M.M. Correia, P. de S. P.M., S.G. M.L., L.H., M. B.I., J.J.G. Moura, Electrochemical studies on c -type cytochromes at microelectrodes, J. Electroanal. Chem. 464 (1999) 76–84.
[71] K. Rabaey, N. Boon, Microbial phenazine production enhances electron transfer in biofuel cells, Environ. Sci. Technol. 39 (2005) 3401–3408.
[72] E. Marsili, D.B. Baron, I.D. Shikhare, D. Coursolle, J.A. Gralnick, D.R. Bond, Shewanella secretes flavins that mediate extracellular electron transfer, Proc. Natl. Acad. Sci. 105 (2008) 6–11, https://doi.org/10.1073/pnas.0710525105.
[73] H. Von Canstein, J. Ogawa, S. Shimizu, J.R. Lloyd, Secretion of flavins by *Shewanella* species and their role in extracellular electron transfer, Appl. Environ. Microbiol. 74 (2008) 615–623, https://doi.org/10.1128/AEM.01387-07.
[74] T. Zhang, C. Cui, S. Chen, H. Yang, P. Shen, The direct electrocatalysis of *Escherichia coli* through electroactivated excretion in microbial fuel cell, Electrochem. Commun. 10 (2008) 293–297, https://doi.org/10.1016/j.elecom.2007.12.009.
[75] A.J. Bard, L.R. Faulkner, Electrochemical Methods: Fundamentals and Applications, John Wiley & Sons, Inc., 2001.
[76] E. Marsili, D.B. Baron, I.D. Shikhare, D. Coursolle, J.A. Gralnick, D.R. Bond, *Shewanella* secretes flavins that mediate extracellular electron transfer, Proc. Natl. Acad. Sci. 105 (10) (2008) 3968–3973.
[77] D.R. Lovley, Microbial fuel cells: novel microbial physiologies and engineering approaches, Curr. Opin. Biotechnol. 17 (2006) 327–332, https://doi.org/10.1016/j.copbio.2006.04.006.
[78] G. Reguera, K.D. Mccarthy, T. Mehta, J.S. Nicoll, M.T. Tuominen, D.R. Lovley, Extracellular electron transfer via microbial nanowires, Nature 435 (2005) 1098–1101, https://doi.org/10.1038/nature03661.
[79] Y.A. Gorby, S. Yanina, J.S. Mclean, K.M. Rosso, D. Moyles, A. Dohnalkova, T. J. Beveridge, I.S. Chang, B.H. Kim, K.S. Kim, D.E. Culley, S.B. Reed, M.F. Romine, D.A. Saffarini, E.A. Hill, L. Shi, D.A. Elias, D.W. Kennedy, G. Pinchuk, K. Watanabe, S. Ishii, B. Logan, K.H. Nealson, J.K. Fredrickson, Electrically conductive bacterial nanowires produced by *Shewanella oneidensis* strain MR-1 and other microorganisms, Proc. Natl. Acad. Sci. 103 (2006), https://doi.org/10.1073/pnas.0604517103.
[80] A.B. Thermincola, P. Parameswaran, T. Bry, S.C. Popat, B.G. Lusk, B.E. Rittmann, Kinetic, electrochemical, and microscopic characterization of the thermophilic, anode-respiring bacterium *Thermincola ferriacetica*, Environ. Sci. Technol. 47 (9) (2013) 4934–4940.
[81] M. Aadil, M. Mahmood, M. Farooq, I.A. Alsafari, S. Zulfiqar, M. Shahid, FlatChem fabrication of MnO 2 nanowires and their nanohybrid with flat conductive matrix for the treatment of industrial effluents, FlatChem 30 (2021) 100316, https://doi.org/10.1016/j.flatc.2021.100316.
[82] T. Lan, C. Wang, T. Sangeetha, Y. Yang, A. Garg, Constructed mathematical model for nanowire electron transfer in microbial fuel cells, J. Power Sources 402 (2018) 483–488, https://doi.org/10.1016/j.jpowsour.2018.09.074.
[83] E. Environ, N.S. Malvankar, T. Tuominen, D.R. Lovley, Lack of cytochrome involvement in long-range electron transport through conductive biofilms and nanowires of *Geobacter sulfurreducens*, Energy Environ. Sci. 5 (2012) 8651–8659, https://doi.org/10.1039/c2ee22330a.
[84] N.S. Malvankar, M. Vargas, K. Nevin, P.L. Tremblay, K. Evans-Lutterodt, D. Nykypanchuk, E. Martz, M.T. Tuomine, D.R. Lovley, Structural basis for metallic-like conductivity in microbial nanowires, MBio 6 (2015), https://doi.org/10.1128/mBio.00084-15.
[85] M. Vargas, N.S. Malvankar, P.L. Tremblay, C. Leang, J.A. Smith, P. Patel, O. Synoeyenbos-West, K.P. Nevin, D.R. Lovley, Aromatic amino acids required for pili conductivity and long-range extracellular electron transport in *Geobacter sulfurreducens*, MBio 4 (2013), https://doi.org/10.1128/mBio.00105-13.
[86] N.S. Malvankar, M. Vargas, K.P. Nevin, A.E. Franks, C. Leang, B.C. Kim, K. Inoue, T. Mester, S.F. Covalla, J.P. Johnson, V.M. Rotello, M.T. Tuominen, D.R. Lovley, Tunable metallic-like conductivity in microbial nanowire networks, Nat. Nanotechnol. 6 (2011) 573–579, https://doi.org/10.1038/nnano.2011.119.
[87] K. Richter, M. Schicklberger, J. Gescher, Dissimilatory reduction of extracellular electron acceptors in anaerobic respiration, Appl. Environ. Microbiol. 78 (2012) 913–921, https://doi.org/10.1128/AEM.06803-11.
[88] L. Shi, K.M. Rosso, T.A. Clarke, D.J. Richardson, J.M. Zachara, J.K. Fredrickson, Molecular underpinnings of Fe(III) oxide reduction by *Shewanella oneidensis* MR-1, Front. Microbiol. 3 (2012), https://doi.org/10.3389/fmicb.2012.00050.
[89] I. Torres, A.K. Marcus, H. Lee, P. Parameswaran, R. Krajmalnik-brown, B. E. Rittmann, A kinetic perspective on extracellular electron transfer by anode-respiring bacteria, FEMS Microbiol. Rev. 34 (2009) 3–17, https://doi.org/10.1111/j.1574-6976.2009.00191.x.
[90] Z. Qiu, F. Cao, G. Pan, C. Li, M. Chen, Y. Zhang, X. He, Y. Xia, X. Xia, W. Zhang, Carbon materials for metal-ion batteries, ChemPhysMater 2 (2023) 267–281, https://doi.org/10.1016/j.chphma.2023.02.002.
[91] B.A. Lim, S. Lim, Y.L. Pang, S.H. Shuit, S.H. Kuan, Critical review on the development of biomass waste as precursor for carbon material as electrocatalysts for metal-air batteries, Renew. Sust. Energ. Rev. 184 (2023) 113451, https://doi.org/10.1016/j.rser.2023.113451.
[92] Z. Zhai, L. Zhang, T. Du, B. Ren, Y. Xu, S. Wang, J. Miao, Z. Liu, A review of carbon materials for supercapacitors, Mater. Des. 221 (2022) 111017, https://doi.org/10.1016/j.matdes.2022.111017.
[93] A. Kumar, E. Singh, R. Mishra, S. Kumar, Biochar as environmental armour and its diverse role towards protecting soil, water and air, Sci. Total Environ. 806 (2022) 150444, https://doi.org/10.1016/j.scitotenv.2021.150444.
[94] C. Kim, S.N. Talapaneni, L. Dai, Porous carbon materials for CO2 capture, storage and electrochemical conversion, Mater. Rep. Energy 3 (2023) 100199, https://doi.org/10.1016/j.matre.2023.100199.
[95] E.C. Kohlrausch, D.D.V. Freitas, C. Inácio, L.F. Loguercio, L.A. Santa-cruz, L. José, L. Maciel, M.Z. Oliveira, C. Indiara, G. Machado, Advances in carbon materials applied to carbon-based perovskite solar cells, Energ. Technol. 2200676 (2023) 1–21, https://doi.org/10.1002/ente.202200676.
[96] M. Toyoda, M. Inagaki, Carbon materials for solar steam-generation, Carbon N. Y. 214 (2023) 118373, https://doi.org/10.1016/j.carbon.2023.118373.
[97] A.A. Yaqoob, M.N.M. Ibrahim, M. Rafatullah, Y.S. Chua, A. Ahmad, K. Umar, Recent advances in anodes for microbial fuel cells: an overview, Materials 13 (2020), https://doi.org/10.3390/ma13092078.
[98] J. Palma, E. Garcia-quismondo, Carbon felt nanoporous oxide coating on carbon paper electrodes to enable bio-hydrogen production in microbial electrolysis cells, Catal. Today 422 (2023), https://doi.org/10.1016/j.cattod.2023.114246.
[99] R. Rossi, J. Nicolas, B.E. Logan, Using nickel-molybdenum cathode catalysts for efficient hydrogen gas production in microbial electrolysis cells, J. Power Sources 560 (2023) 232594, https://doi.org/10.1016/j.jpowsour.2022.232594.
[100] D. Liu, X. An, P. Wang, X. Ma, Y. Zhao, An effective copper doping strategy of Co (OH)F cathode for producing hydrogen in microbial electrolytic cells, Int. J. Hydrog. Energy 48 (2023) 26072–26083, https://doi.org/10.1016/j.ijhydene.2023.03.331.
[101] S. Lu, B. Lu, G. Tan, W. Moe, W. Xu, Y. Wang, D. Xing, X. Zhu, Mo2N nanobelt cathodes for efficient hydrogen production in microbial electrolysis cells with shaped biofilm microbiome, Biosens. Bioelectron. 167 (2020) 112491, https://doi.org/10.1016/j.bios.2020.112491.

[102] D. Zheng, W. Gu, Q. Zhou, L. Zhang, C. Wei, Ammonia oxidation and denitrification in a bio-anode single-chambered microbial electrolysis cell, Bioresour. Technol. 310 (2020) 123466, https://doi.org/10.1016/j.biortech.2020.123466.
[103] T.H.J.A. Sleutels, H.V.M. Hamelers, C.J.N. Buisman, Effect of mass and charge transport speed and direction in porous anodes on microbial electrolysis cell performance, Bioresour. Technol. 102 (2011) 399–403, https://doi.org/10.1016/j.biortech.2010.06.018.
[104] G. Rani, K. Krishna, K.N. Yogalakshmi, Enhancing the electrochemical performance of Fe3O4 nanoparticles layered carbon electrodes in microbial electrolysis cell, J. Environ. Chem. Eng. 9 (2021) 106326, https://doi.org/10.1016/j.jece.2021.106326.
[105] K. Hagos, C. Liu, X. Lu, Effect of endogenous hydrogen utilization on improved methane production in an integrated microbial electrolysis cell and anaerobic digestion: employing catalyzed stainless steel mesh cathode, Chin. J. Chem. Eng. 26 (2018) 574–582, https://doi.org/10.1016/j.cjche.2017.08.005.
[106] S. Rozenfeld, H. Teller, M. Schechter, R. Farber, O. Krichevski, A. Schechter, R. Cahan, Exfoliated molybdenum di-sulfide (MoS2) electrode for hydrogen production in microbial electrolysis cell, Bioelectrochemistry 123 (2018) 201–210, https://doi.org/10.1016/j.bioelechem.2018.05.007.
[107] H. Yuan, L. Deng, X. Qian, L. Wang, D. Li, Significant enhancement of electron transfer from *Shewanella oneidensis* using a porous N-doped carbon cloth in a bioelectrochemical system, Sci. Total Environ. 665 (2019) 882–889, https://doi.org/10.1016/j.scitotenv.2019.02.082.
[108] L. Huang, W. Kong, S. Song, X. Quan, G. Li, Treatment of industrial etching terminal wastewater using ZnFe 2 O 4/g-C 3 N 4 heterojunctions photo-assisted cathodes in single-chamber microbial electrolysis cells, Appl. Catal. B 335 (2023) 122849, https://doi.org/10.1016/j.apcatb.2023.122849.
[109] S. Song, L. Huang, P. Zhou, Efficient H2 production in a ZnFe2O4/g-C3N4 photo-cathode single-chamber microbial electrolysis cell, Appl. Microbiol. Biotechnol. (2023) 391–404, https://doi.org/10.1007/s00253-022-12293-3.
[110] T. Jayabalan, Enhanced biohydrogen production from sugar industry effluent using nickel oxide and cobalt oxide as cathode nanocatalysts in microbial electrolysis cell, Int. J. Energy Res. (2021) 17431–17439, https://doi.org/10.1002/er.5645.
[111] T. Jayabalan, M. Matheswaran, T.K. Radhakrishnan, Influence of nickel molybdate nanocatalyst for enhancing biohydrogen production in microbial electrolysis cell utilizing sugar industrial effluent, Bioresour. Technol. 320 (2021) 124284, https://doi.org/10.1016/j.biortech.2020.124284.
[112] K. Kim, S.E. Habas, J.A. Schaidle, B.E. Logan, Application of phase-pure nickel phosphide nanoparticles as cathode catalysts for hydrogen production in microbial electrolysis cells, Bioresour. Technol. 293 (2019) 122067, https://doi.org/10.1016/j.biortech.2019.122067.
[113] A. Kumar, R. Shankar, P. Mondal, Effects of nickle, nickle-cobalt and nickle-cobalt-phosphorus nanocatalysts for enhancing biohydrogen production in microbial electrolysis cells using paper industry wastewater change in chemical oxygen demand, J. Environ. Manag. 298 (2021) 113542, https://doi.org/10.1016/j.jenvman.2021.113542.
[114] L. Wang, Y. Chen, Y. Ye, B. Lu, S. Zhu, S. Shen, Evaluation of low-cost cathode catalysts for high yield biohydrogen production in microbial electrolysis cell, Water Sci. Technol. (2011) 440–448, https://doi.org/10.2166/wst.2011.241.
[115] W. Cai, W. Liu, H. Sun, J. Li, L. Yang, M. Liu, S. Zhao, Ni5P4-NiP2 nanosheet matrix enhances electron-transfer kinetics for hydrogen recovery in microbial electrolysis cells, Appl. Energy 209 (2018) 56–64, https://doi.org/10.1016/j.apenergy.2017.10.082.
[116] M. Siegert, M.D. Yates, A.M. Spormann, B.E. Logan, Methanobacterium dominates biocathodic archaeal communities in methanogenic microbial electrolysis cells, ACS Sustain. Chem. Eng. (2015), https://doi.org/10.1021/acssuschemeng.5b00367.
[117] S.M. Parsa, Z. Chen, S. Feng, Y. Yang, L. Luo, H. Hao, Metal-free nitrogen-doped carbon-based electrocatalysts for oxygen reduction reaction in microbial fuel cells: advances, challenges, and future directions, Nano Energy 134 (2025), https://doi.org/10.1016/j.nanoen.2024.110537.
[118] C. Bi, Q. Wen, Y. Chen, H. Xu, Boosting power output in microbial fuel cell with sulfur - doped MXene/polypyrrole hydrogel anode for enhanced extracellular electron transfer process, J. Appl. Electrochem. 54 (2024) 2729–2743, https://doi.org/10.1007/s10800-024-02137-5.
[119] L. Yang, Q. Wen, Y. Chen, C. Lin, H. Gao, Z. Qiu, Capacitive bio–electrocatalyst Mxene@CoMo–ZIF sulfide heterostructure for boosted biofilm electroactivity to enhance renewable energy conversion, Renew. Energy 243 (2025) 122545, https://doi.org/10.1016/j.renene.2025.122545.
[120] F. Sun, Y. Chen, Q. Wen, Y. Yang, Co-doped modified microbial fuel cell promote sulfamethoxine degradation with high enrichment of electroactive bacteria and extracellular electron transfer, Renew. Energy 232 (2024) 121091, https://doi.org/10.1016/j.renene.2024.121091.
[121] X. Fu, X. Pan, Q. Wen, Y. Chen, C. Lin, H. Gao, Z. Qiu, L. Yang, H. Xu, Enhancing direct electron transfer process and power generation in microbial fuel cell using anode of molybdenum-based ternary material, Int. J. Hydrog. Energy 93 (2024) 1205–1217, https://doi.org/10.1016/j.ijhydene.2024.10.435.
[122] S. Wang, D. Zhao, Z. Qiu, G. Zhang, C. Lin, 3D porous carbon materials in situ-embedded with Fe3C/Fe nanoparticles as high-performance anode electrocatalysts of microbial fuel cells, J. Environ. Chem. Eng. 13 (2025) 116171, https://doi.org/10.1016/j.jece.2025.116171.
[123] Y. Meng, X. Pan, Y. Chen, Q. Wen, C. Lin, H. Gao, Z. Qiu, L. Yang, The enhancement of extracellular electron transfer processes through the design of biomimetic grape-like materials, J. Environ. Chem. Eng. 13 (2025) 115484, https://doi.org/10.1016/j.jece.2025.115484.
[124] X. Zhu, Z. Qiu, J. Liu, S. Wang, Y. Chen, K. Liu, T. Liu, C. Lin, Enhanced power generation by carbonized microsphere embedded with bimetallic carbides nanoparticles as efficient electrocatalyst in bioenergy harvesting systems, J. Power Sources 624 (2024) 235552, https://doi.org/10.1016/j.jpowsour.2024.235552.
[125] X. Pan, Y. Chen, Q. Wen, C. Lin, H. Gao, Z. Qiu, L. Yang, Synergistic effect of bimetallic bioelectrocatalysis and endogenous soluble electron mediators for functional regulation of electroactive biofilms, J. Clean. Prod. 491 (2025).
[126] X. Zhu, Y. Gao, Y. Chen, Q. Wen, J. Yin, Insight into the enhancing mechanism of extracellular electron transfer on ordered sulfur exposure using frozen-ultraviolet irradiation, J. Power Sources 631 (2025) 236212, https://doi.org/10.1016/j.jpowsour.2025.236212.
[127] X. Pu, Y. Wu, J. Liu, B. Wu, 3D bioprinting of microbial-based living materials for advanced energy and environmental applications, Chem Bio Eng. 1 (2024) 568–592, https://doi.org/10.1021/cbe.4c00024.
[128] M.S. Bhagat, C. Mevada, J. Shah, M.A. Rasheed, M. Mäntysalo, Zero-discharge, self-sustained 3D-printed microbial electrolysis cell for biohydrogen production: a review, Chem. Commun. 61 (2025) 5410–5421, https://doi.org/10.1039/d5cc00103j.
[129] T.H. Chung, B.R. Dhar, A mini-review on applications of 3D printing for microbial electrochemical technologies, Front. Energy Res. 9 (2021), https://doi.org/10.3389/fenrg.2021.679061.
[130] B. Bian, D. Shi, X. Cai, M. Hu, Q. Guo, C. Zhang, Q. Wang, A.X. Sun, J. Yang, 3D printed porous carbon anode for enhanced power generation in microbial fuel cell, Nano Energy 44 (2018) 174–180, https://doi.org/10.1016/j.nanoen.2017.11.070.
[131] B. Bian, C. Wang, M. Hu, Z. Yang, X. Cai, D. Shi, J. Yang, Application of 3D printed porous copper anode in microbial fuel cells, Front. Energy Res. 6 (2018), https://doi.org/10.3389/fenrg.2018.00050.
[132] H. Li, L. Zhang, R. Wang, J. Sun, Y. Qiu, S. Liu, 3D hierarchical porous carbon foams as high-performance free-standing anodes for microbial fuel cells, EcoMat 5 (2023), https://doi.org/10.1002/eom2.12273.
[133] A. Miller, L. Singh, L. Wang, H. Liu, Linking internal resistance with design and operation decisions in microbial electrolysis cells, Environ. Int. 126 (2019) 611–618, https://doi.org/10.1016/j.envint.2019.02.056.
[134] B.P. Cario, R. Rossi, K. Kim, B.E. Logan, Applying the electrode potential slope method as a tool to quantitatively evaluate the performance of individual microbial electrolysis cell components, Bioresour. Technol. 287 (2019) 121418, https://doi.org/10.1016/j.biortech.2019.121418.
[135] L. Rago, N. Monpart, P. Cortés, J.A. Baeza, A. Guisasola, Performance of microbial electrolysis cells with bioanodes grown at different external resistances, Water Sci. Technol. (2016) 1129–1135, https://doi.org/10.2166/wst.2015.418.
[136] F. Bas, 3D printed anode electrodes for microbial electrolysis cells, Fuel 317 (2022).
[137] E. Roubaud, B. Erable, L. Etcheverry, A. Bergel, S. Da, Design of 3D microbial anodes for microbial electrolysis cells (MEC) fuelled by domestic wastewater. Part I: multiphysics modelling, J. Environ. Chem. Eng. 9 (2021), https://doi.org/10.1016/j.jece.2021.105476.
[138] S. Luo, X. Zhu, B. Fu, F. Liu, L. Sun, K. He, H. Yang, X. Zhang, X. Huang, Outstanding energy reduction of nitrogen recovery by biohythane concept introduction by 3D-weaved anode network in microbial electrolysis cell, Resour. Conserv. Recycl. 188 (2023).
[139] V. Kumar, M. Prasad Behera, Y. Lv, B. Pradheepa Kamarajan, S. Singamneni, Hydrogen production from wastewater using interdigitated printed electrode-based single-chamber microbial electrolysis cells, Mater. Des. 245 (2024), https://doi.org/10.1016/j.matdes.2024.113237.
[140] S.M. Parsa, Z. Chen, H.H. Ngo, W. Wei, X. Zhang, Y. Liu, B.J. Ni, W. Guo, 15 years of progress on transition metal-based electrocatalysts for microbial electrochemical hydrogen production: from nanoscale design to macroscale application, Nano Lett. 17 (2025), https://doi.org/10.1007/s40820-025-01781-6.
[141] Z. Guo, Z. Liu, D. Li, B. Zhao, X. Zhang, Y. Duan, Z. He, W. Liu, X. Yue, A. Zhou, Sacrificial iron anode contributes to ferrous release and electron transfer via microbial electrolysis cell: enhancing hydrogen and vivianite recovery from waste activated sludge, Chem. Eng. J. 522 (2025), https://doi.org/10.1016/j.cej.2025.167429.
[142] X. Li, R. Zhang, Y. Qian, I. Angelidaki, Y. Zhang, The impact of anode acclimation strategy on microbial electrolysis cell treating hydrogen fermentation effluent, Bioresour. Technol. 236 (2017) 37–43, https://doi.org/10.1016/j.biortech.2017.03.160.
[143] M.L. Ullery, B.E. Logan, Anode acclimation methods and their impact on microbial electrolysis cells treating fermentation effluent, Int. J. Hydrog. Energy 40 (2015) 6782–6791, https://doi.org/10.1016/j.ijhydene.2015.03.101.
[144] L. Gil-carrera, P. Mehta, A. Escapa, A. Morán, V. García, S.R. Guiot, B. Tartakovsky, Optimizing the electrode size and arrangement in a microbial electrolysis cell, Bioresour. Technol. 102 (2011) 9593–9598, https://doi.org/10.1016/j.biortech.2011.08.026.
[145] D. Liang, S. Peng, S. Lu, Y. Liu, F. Lan, Y. Xiang, Enhancement of hydrogen production in a single chamber microbial electrolysis cell through anode arrangement optimization, Bioresour. Technol. 102 (2011) 10881–10885, https://doi.org/10.1016/j.biortech.2011.09.028.
[146] J. Zhang, Y. Bai, Y. Fan, H. Hou, Improved bio-hydrogen production from glucose by adding a specific methane inhibitor to microbial electrolysis cells with a

double anode arrangement, J. Biosci. Bioeng. 122 (2016) 488–493, https://doi.org/10.1016/j.jbiosc.2016.03.016.
[147] X. Li, D. Liang, Y. Bai, Y. Fan, Enhanced H2 production from corn stalk by integrating dark fermentation and single chamber microbial electrolysis cells with double anode arrangement, Int. J. Hydrog. Energy 39 (2014) 8977–8982, https://doi.org/10.1016/j.ijhydene.2014.03.065.
[148] G. Baek, R. Rossi, B.E. Logan, Changes in electrode resistances and limiting currents as a function of microbial electrolysis cell reactor configurations, Electrochim. Acta 388 (2021) 138590, https://doi.org/10.1016/j.electacta.2021.138590.
[149] L. Wang, K. Linowski, H. Liu, Scalable membrane-less microbial electrolysis cell with multiple compact electrode assemblies for high performance hydrogen production, Chem. Eng. J. 454 (2023), https://doi.org/10.1016/j.cej.2022.140257.
[150] Z. Guo, S. Thangavel, L. Wang, Z. He, W. Cai, A. Wang, W. Liu, Efficient methane production from beer wastewater in a membraneless microbial electrolysis cell with a stacked cathode: the effect of the cathode/anode ratio on bioenergy recovery, Energy Fuel (2017), https://doi.org/10.1021/acs.energyfuels.6b02375.
[151] S. Cheng, B.E. Logan, High hydrogen production rate of microbial electrolysis cell (MEC) with reduced electrode spacing, Bioresour. Technol. 102 (2011) 3571–3574, https://doi.org/10.1016/j.biortech.2010.10.025.
[152] E.U. Fonseca, K. Kim, R. Rossi, B.E. Logan, Improving microbial electrolysis stability using flow-through brush electrodes and monitoring anode potentials relative to thermodynamic minima, Int. J. Hydrog. Energy 46 (2021) 9514–9522, https://doi.org/10.1016/j.ijhydene.2020.12.102.
[153] S. Rozenfeld, B. Gandu, L. Ouaknin, I. Dubrovin, A. Schechter, Hydrogen production in a semi-single-chamber microbial electrolysis cell based on anode encapsulated in a dialysis bag, Int. J. Energy Res. (2021) 1–15, https://doi.org/10.1002/er.7050.
[154] B. Gandu, S. Rozenfeld, L. Ouaknin, A. Schechter, R. Cahan, Immobilization of bacterial cells on carbon-cloth anode using alginate for hydrogen generation in a microbial electrolysis cell, J. Power Sources 455 (2020) 227986, https://doi.org/10.1016/j.jpowsour.2020.227986.
[155] I.A. Dubrovin, L.O. Hirsch, S. Rozenfeld, B. Gandu, O. Menashe, A. Schechter, R. Cahan, Hydrogen production in microbial electrolysis cells based on bacterial anodes encapsulated in a small bioreactor platform, Microorganisms 10 (5) (2022) 1007.
[156] I.A. Dubrovin, L.O. Hirsch, A. Chiliveru, A. Jukanti, S. Rozenfeld, A. Schechter, R. Cahan, Microbial electrolysis cells based on a bacterial anode encapsulated with a dialysis bag including graphite particles, Microorganisms 12 (2024), https://doi.org/10.3390/microorganisms12071486.
[157] L.O. Hirsch, B. Gandu, A. Chiliveru, I.A. Dubrovin, A. Jukanti, A. Schechter, R. Cahan, Hydrogen production in microbial electrolysis cells using an alginate hydrogel bioanode encapsulated with a filter bag, Polymers (Basel) 16 (2024), https://doi.org/10.3390/polym16141996.
[158] S. Chavan, A. Gaikwad, Hydrogen generation from bamboo biomass using enzymatic hydrolysis and subsequent microbial electrolysis in a single chamber microbial electrolysis cell, Biochem. Eng. J. 193 (2023) 108853, https://doi.org/10.1016/j.bej.2023.108853.
[159] B.S. Zakaria, S. Barua, A. Sharaf, Y. Liu, B.R. Dhar, Impact of antimicrobial silver nanoparticles on anode respiring bacteria in a microbial electrolysis cell, Chemosphere 213 (2018) 259–267, https://doi.org/10.1016/j.chemosphere.2018.09.060.
[160] M.I. San-martín, A. Escapa, R.M. Alonso, M. Canle, A. Morán, Degradation of 2-mercaptobenzothizaole in microbial electrolysis cells: intermediates, toxicity, and microbial communities, Sci. Total Environ. 733 (2020) 139155, https://doi.org/10.1016/j.scitotenv.2020.139155.
[161] S. Xu, H. Liu, Y. Fan, Enhanced performance and mechanism study of microbial electrolysis cells using Fe nanoparticle-decorated anodes, Appl. Microbiol. Biotechnol. (2012) 871–880, https://doi.org/10.1007/s00253-011-3643-2.
[162] P. Liu, P. Liang, Y. Jiang, W. Hao, B. Miao, D. Wang, X. Huang, Stimulated electron transfer inside electroactive bio film by magnetite for increased performance microbial fuel cell, Appl. Energy 216 (2018) 382–388, https://doi.org/10.1016/j.apenergy.2018.01.073.
[163] J. Zhang, Y. Zhang, X. Quan, S. Chen, Effects of ferric iron on the anaerobic treatment and microbial biodiversity in a coupled microbial electrolysis cell (MEC) - anaerobic reactor, Water Res. 47 (2013) 5719–5728, https://doi.org/10.1016/j.watres.2013.06.056.
[164] J. Hu, C. Zeng, G. Liu, H. Luo, L. Qu, R. Zhang, Magnetite nanoparticles accelerate the autotrophic sulfate reduction in biocathode microbial electrolysis cells, Biochem. Eng. J. 133 (2018) 96–105, https://doi.org/10.1016/j.bej.2018.01.036.
[165] A.Y. Goren, A.F. Kilicaslan, I. Dincer, A. Khalvati, Hydrogen production from energetic poplar and waste sludge by electrohydrogenesis using membraneless microbial electrolysis cells, Renew. Energy 237 (2024), https://doi.org/10.1016/j.renene.2024.121750.
[166] Z. Ying, S. Li, Y. Zhou, J. Zhao, Y. Shen, J. Ye, S. Zhang, X. Weng, J. Chen, Polypyrrole/cellulose-based carbon aerogel anode for enhanced toluene removal in microbial electrolysis cells, Chem. Eng. J. 522 (2025), https://doi.org/10.1016/j.cej.2025.167259.
[167] L. Wang, K. Linowski, M.D.Z. Islam, H. Harrison, C. Yu, H. Liu, Efficient hydrogen production from low-conductivity high-strength wastewater without buffer addition using compact electrode assemblies in membraneless microbial electrolysis cells, Chem. Eng. J. 519 (2025), https://doi.org/10.1016/j.cej.2025.165062.
[168] Y. Zhu, H. Tang, D. Liang, S. Liu, N. Wang, F. Huang, W. He, Y. Feng, Highly conductive PBFDO network bridging biofilm and electrode interface for electron capture and transfer in microbial electrochemical system, Chem. Eng. J. 520 (2025), https://doi.org/10.1016/j.cej.2025.166160.
[169] X. Wu, D. Sun, M. Li, X. Zhang, N.A. Al-Dhabi, Q. Fang, W. Tang, Q. Tang, J. Kou, Z. Wang, X. Zhang, Y. Hua, T. Cai, Nano-Fe3O4/polymerize aniline/carbon cathode based microbial fuel cell for efficient power generation and uranium separation, Chem. Eng. J. 487 (2024), https://doi.org/10.1016/j.cej.2024.150634.
[170] H. Seelajaroen, S. Spiess, M. Haberbauer, M.M. Hassel, A. Aljabour, S. Thallner, G. M. Guebitz, N.S. Sariciftci, Enhanced methane producing microbial electrolysis cells for wastewater treatment using poly(neutral red) and chitosan modified electrodes, Sustain. Energy Fuel 4 (2020) 4238–4248, https://doi.org/10.1039/d0se00770f.
[171] D. Rahmadita, T.S. Utami, R. Arbianti, Modification of anodes with polyaniline coating in microbial electrolysis cell system to reduce ammonia concentration in fertilizer plant liquid waste, in: AIP Conf Proc, American Institute of Physics Inc., 2021, https://doi.org/10.1063/5.0063927.
[172] T. Guo, C. Zhang, J. Zhao, C. Ma, S. Li, W. Li, Evaluation of polypyrrole-modified bioelectrodes in a chemical absorption-bioelectrochemical reduction integrated system for NO removal, Sci. Rep. 9 (2019), https://doi.org/10.1038/s41598-019-49610-2.
[173] K. Feng, Y. Lu, Y. Shen, S. Zhang, J. Ye, J. Chen, J. Zhao, Multilayered structure and activity of electroactive biofilms in response to the switch from microbial fuel cell to microbial electrolysis cell, J. Power Sources 587 (2023), https://doi.org/10.1016/j.jpowsour.2023.233704.
[174] K.P. Kumar, A.S. Kundar, K.J. Abhijith, H. Gowda, U.S. Meda, M.A.L.A. Raj, J. H. Patil, Development of polymeric layer on anode for enhanced hydrogen generation in microbial electrolysis cell, Asian J. Chem. (2017) 226–228, https://doi.org/10.14233/ajchem.2017.20382 (Chemical Publishing Co.).
[175] Y. Li, Y. Zhang, O. Wang, W. Kong, S. Tabassum, Anodic modification-enhanced microbial electrolysis cell coupled with anaerobic digestion for coal gasification wastewater treatment, Biochem. Eng. J. 220 (2025), https://doi.org/10.1016/j.bej.2025.109767.
[176] C. Yang, Z. Liu, N. Fang, W. Yu, C. Li, Y. Chu, Fe-doped biochars prepared via hydrothermal treatment and low-temperature air calcination to activate peroxymonosulfate for efficient tetracycline degradation, Water Cycle 6 (2025) 1–12, https://doi.org/10.1016/j.watcyc.2024.06.003.
[177] Y. Wei, B. Fang, R. Tang, J. Guo, H. Shen, K. Yan, C. He, Y. Qin, J. Zhang, Key role of C–O–Fe in coal gasification slag-derived carbon–iron composites for peroxymonosulfate activation for 2,4-dichlorophenol degradation, Sep. Purif. Technol. 380 (2026), https://doi.org/10.1016/j.seppur.2025.135327.
[178] L. Qin, L. Liang, Y. Qi, Y. Li, F. Yin, X. Zhao, A novel high-oxygen-evolution anode boosts microbial electrolysis for perfluorooctanoic acid removal, Desalination Water Treat 323 (2025), https://doi.org/10.1016/j.dwt.2025.101291.
[179] P. Kosse, M. Lübken, M. Wichern, Selective inhibition of methanogenic archaea in leach bed systems by sodium 2-bromoethanesulfonate, Environ. Technol. Innov. 5 (2016) 199–207, https://doi.org/10.1016/j.eti.2016.03.003.
[180] L. Zhuang, Q. Chen, S. Zhou, Y. Yuan, H. Yuan, Methanogenesis control using 2-bromoethanesulfonate for enhanced power recovery from sewage sludge in air-cathode microbial fuel cells. www.electrochemsci.org, 2012.
[181] S.G. Park, C. Rhee, S.G. Shin, J. Shin, H.O. Mohamed, Y.J. Choi, K.J. Chae, Methanogenesis stimulation and inhibition for the production of different target electrobiofuels in microbial electrolysis cells through an on-demand control strategy using the coenzyme M and 2-bromoethanesulfonate, Environ. Int. 131 (2019), https://doi.org/10.1016/j.envint.2019.105006.
[182] K.J. Chae, M.J. Choi, K.Y. Kim, F.F. Ajayi, I.S. Chang, I.S. Kim, Selective inhibition of methanogens for the improvement of biohydrogen production in microbial electrolysis cells, Int. J. Hydrog. Energy 35 (2010) 13379–13386, https://doi.org/10.1016/j.ijhydene.2009.11.114.
[183] T. Catal, K.L. Lesnik, H. Liu, Suppression of methanogenesis for hydrogen production in single-chamber microbial electrolysis cells using various antibiotics, Bioresour. Technol. 187 (2015) 77–83, https://doi.org/10.1016/j.biortech.2015.03.099.
[185] R. Cahan, Improvement of microbial electrolysis cell plasma-pretreated carbon cloth and stainless steel, Energies 12 (10) (2019) 1968.
[186] Y. Hou, H. Luo, G. Liu, R. Zhang, J. Li, S. Fu, Improved hydrogen production in the microbial electrolysis cell by inhibiting methanogenesis using ultraviolet irradiation, Environ. Sci. Technol. 48 (2014) 10482–10488, https://doi.org/10.1021/es501202e.
[187] A. Nandy, V. Kumar, P.P. Kundu, Effect of electric impulse for improved energy generation in mediatorless dual chamber microbial fuel cell through electroevolution of *Escherichia coli*, Biosens. Bioelectron. 79 (2016) 796–801, https://doi.org/10.1016/j.bios.2016.01.023.
[188] R.B. Al-Mayyahi, S.G. Park, D.A. Jadhav, M. Hussien, H. Omar Mohamed, P. Castaño, S.Y. Al-Qaradawi, K.J. Chae, Unraveling the influence of magnetic field on microbial and electrogenic activities in bioelectrochemical systems: a comprehensive review, Fuel 331 (2023), https://doi.org/10.1016/j.fuel.2022.125889.
[189] H. Harrison, L. Wang, H. Liu, Tackling hydrogen scavengers via temporal electrochemical shock using dual-functional electrodes in single-chamber

microbial electrolysis cells, Chem. Eng. J. 522 (2025), https://doi.org/10.1016/j.cej.2025.167126.

[190] S.G. Park, C. Rhee, D.A. Jadhav, J.H. Jang, M.H. Hwang, K.J. Chae, Enhanced hydrogen production in microbial electrolysis cells through a magnetically induced electroactive anode biofilm, Chem. Eng. J. 505 (2025), https://doi.org/10.1016/j.cej.2024.159071.

[191] S.M. Parsa, F. Norozpour, S. Momeni, S. Shoeibi, X. Zeng, Z. Said, W. Guo, H. H. Ngo, B.J. Ni, Advanced nanostructured materials in solar interfacial steam generation and desalination against pathogens: combatting microbial-contaminants in water - a critical review, J. Mater. Chem. A Mater. 11 (2023) 18046–18080, https://doi.org/10.1039/d3ta03343k.